by removal of one CO. Low-temperature accumulation of axial-^{13}CO-$Os_3(CO)_{11}(^{13}CO)$ is consistent with the IR spectral characterization of the accumulated $Os_3(CO)_{11}$ precursor as an axially vacant fragment. The low-temperature reaction of axially vacant $Os_3(CO)_{11}$ with ^{13}CO to yield axial-^{13}CO-$Os_3(CO)_{11}(^{13}CO)$ has provided an opportunity to characterize the two possible isomers of $Os_3(CO)_{11}(^{13}CO)$.

Electronic factors are likely to control the thermodynamic preference for an axial vacancy in $Os_3(CO)_{11}$. The axial Os-CO bonds in $Os_3(CO)_{12}$[49] are lengthened relative to the equatorial Os-CO bonds due to a greater competition between two axial CO's than between an equatorial CO and a *trans*-Os atom for back donation of electron density from the t_{2g} orbitals of a given Os. This trend in Os-CO bonding extends to the crystallographically characterized axially substituted $Os_3(CO)_{11}(NCMe)$,[50] where, in addition, the axial Os-CO distance trans to the MeCN is the shortest metal-ligand bond distance in the structure. The trans axial CO receives most of the back-donated electron density from the Os orbital, since it is in direct competition with the MeCN, which is a good σ-donor but a poor π-acceptor. For sterically nondemanding entering groups, substitution of CO by weak π-acceptor ligands (CNMe, NCMe, C_5H_5N)[43] favors an axial coordination site trans to CO rather than an equatorial site trans to an Os-Os bond, thus maximizing π bonding with the remaining CO ligands. A "vacancy", having no π-acceptor properties, is similarly expected to reside in an axial site in photogenerated $Os_3(CO)_{11}$, as observed. The $Os_3(CO)_{11}(N_2)$ complex is axially substituted in accord with this trend. The strong π-acid C_2H_4, however, prefers to coordinate equatorially.

Acknowledgment. We thank the National Science Foundation for support of this research.

Registry No. $Os_3(CO)_{12}$, 15696-40-9; $Os_3(CO)_{11}$, 108345-48-8; $Os_3(CO)_{11}(PPh_3)$, 30173-88-7; $Os_3(CO)_{11}(P(OMe)_3)$, 66098-55-3; $Os(CO)_4(PPh_3)$, 21192-24-5; $Os_3(CO)_{11}(N_2)$, 108345-49-9; $Os_3(CO)_{11}(C_2H_4)$, 65772-73-8; $Os_3(CO)_{11}$(2-MeTHF), 108345-50-2; $Os_3(CO)_{11}(C_5H_{10})$, 108345-51-3; $H_2Os_3(CO)_{10}$, 41766-80-7; $H_2Os_3(CO)_{11}$, 56398-24-4; $Os_3(CO)_{11}(^{13}CO)$, 15696-40-9; axial-$Os_3(CO)_{11}(^{13}CO)$, 73346-54-0; equitorial-$Os_3(CO)_{11}(^{13}CO)$, 73295-94-0; $P(OMe)_3$, 121-45-9; PPh_3, 603-35-0; 2-MeTHF, 96-47-9; ^{13}CO, 1641-69-6; CO, 630-08-0; C_2H_4, 74-85-1; N_2, 7727-37-9; H_2, 1333-74-0; 1-pentene, 109-67-1.

Supplementary Material Available: IR and UV-vis spectral data for relevant complexes to supplement Table I and figures showing IR spectral data for the thermal reactions of photogenerated $Os_3(CO)_{11}$ with PPh_3 and with H_2 (6 pages). Ordering information is given on any current masthead page.

Wavelength-, Medium-, and Temperature-Dependent Competition between Photosubstitution and Photofragmentation in $Ru_3(CO)_{12}$ and $Fe_3(CO)_{12}$: Detection and Characterization of Coordinatively Unsaturated $M_3(CO)_{11}$ Complexes

James G. Bentsen and Mark S. Wrighton*

Contribution from the Department of Chemistry, Massachusetts Institute of Technology, Cambridge, Massachusetts 02139. *Received July 8, 1986*

Abstract: Irradiation of 0.1 mM $Ru_3(CO)_{12}$ (λ = 313 nm) or 0.02 mM $Fe_3(CO)_{12}$ (λ = 366 nm) in a methylcyclohexane or 2-methyltetrahydrofuran (2-MeTHF) glass at 90 K yields loss of one CO as the only IR detectable photoreaction to yield products formulated as $M_3(CO)_{11}$ or $M_3(CO)_{11}$(2-MeTHF), respectively. An initially observed axially vacant form of $Ru_3(CO)_{11}$ (II) having no bridging CO's rearranges at 90 K to an axially vacant form (III), having at least one bridging CO, also adopted by $Fe_3(CO)_{11}$ in an alkane glass. An initially observed, equatorially substituted form of $Ru_3(CO)_{11}$(2-MeTHF) (I') rearranges at 90 K to III or a 2-MeTHF adduct of III. I' is extremely photosensitive with respect to further substitution by 2-MeTHF for up to three CO ligands. $Ru_3(CO)_{11}$ (III) reacts with N_2 or ^{13}CO to yield $Ru_3(CO)_{11}(N_2)$ or axial-^{13}CO-$Ru_3(CO)_{11}(^{13}CO)$ complexes, respectively. $Ru_3(CO)_{11}$ and $Fe_3(CO)_{11}$ react with C_2H_4 to yield $M_3(CO)_{11}(C_2H_4)$ complexes. $M_3(CO)_{11}$ (III) reacts with PPh_3 to yield $Ru_3(CO)_{11}(PPh_3)$ at 298 K and $Fe_3(CO)_{11}(PPh_3)$ at 195 K. Long wavelength excitation of $Ru_3(CO)_{12}$ (λ = 366 nm) or $Fe_3(CO)_{12}$ (λ = 436 nm) yields negligible photochemistry in alkane or 2-MeTHF glasses but yields associative photosubstitution of C_2H_4, C_5H_{10}, and ^{13}CO but not N_2 or 2-MeTHF for CO at 90 K. Long wavelength ($\lambda > 540$ nm) excitation of $Fe_3(CO)_{12}$ yields no photochemistry at 90 K but gives asymmetric fragmentation in C_2H_4-containing alkane solutions at 298 K to yield 1 equiv each of $Fe(CO)_5$, $Fe(CO)_4(C_2H_4)$, and $Fe(CO)_3(C_2H_4)_2$; competitive photosubstitution occurs in the presence of PPh_3 to yield $Fe_3(CO)_{11}(PPh_3)$. At 195 K, the $Fe_3(CO)_{11}L/Fe(CO)_{5-n}(L)_n$ (L = C_2H_4, PPh_3; n = 0-2) product ratios increase with decreasing irradiation wavelength. Long wavelength ($\lambda > 420$ nm) irradiation of 0.2 mM $Ru_3(CO)_{12}$ in 195 K alkane solutions containing excess L = CO or C_2H_4 initially yields 1 equiv each of $Ru(CO)_4L$ and $Ru_2(CO)_8L$; $Ru_2(CO)_8(C_2H_4)$ fragments at 195 K to yield 2 more equiv of $Ru(CO)_4(C_2H_4)$. Long wavelength irradiation of $Ru_3(CO)_{12}$ in PPh_3-containing solutions at 195 K yields conversion to a CO-bridged product which reacts thermally at 195 K to form $Ru_3(CO)_{11}(PPh_3)$, in competition with $Ru_3(CO)_{12}$ regeneration; $Ru(CO)_4(PPh_3)$ and $Ru(CO)_3(PPh_3)_2$ are only observed as secondary photoproducts at 195 K. The low-temperature photochemistry of $Ru_3(CO)_{12}$ is discussed in terms of a wavelength-dependent competition between dissociative loss of equatorial CO from higher energy excitation and generation of a nonradical, reactive isomer of $Ru_3(CO)_{12}$ from long wavelength excitation. Implications of the new results for the photocatalyzed isomerization of 1-pentene to *cis*- and *trans*-2-pentene by $M_3(CO)_{12}$ (M = Ru, Fe) precursors are discussed.

This article reports results concerning the photochemical generation of reactive intermediates from visible and near-UV irradiation of $M_3(CO)_{12}$ (M = Fe, Ru) in low-temperature fluid solutions and in rigid organic solvents. A wavelength, medium, and temperature dependent competition between dissociative loss of CO and fragmentation enables selective photogeneration of coordinatively unsaturated $M_3(CO)_{11}$ (M = Fe, Ru) fragments with near-UV irradiation of $M_3(CO)_{12}$ in methylcyclohexane glasses according to eq 1 or, alternatively, reactive dinuclear Ru adducts of π-acceptor ligands (L = CO and C_2H_4) but not PPh_3 with visible light irradiation of $Ru_3(CO)_{12}$ in low-temperature alkane solutions according to eq 2.

0002-7863/87/1509-4530$01.50/0

$$M_3(CO)_{12} \xrightarrow[M = Fe, Ru]{h\nu, 90\ K} M_3(CO)_{11} + CO \quad (1)$$

$$Ru_3(CO)_{12} \xrightarrow[L = CO, C_2H_4]{h\nu, 195\ K} Ru(CO)_4L + Ru_2(CO)_8L \quad (2)$$

Interest in a detailed understanding of the photofragmentation of $M_3(CO)_{12}$ clusters stems from olefin isomerization activity initiated at elevated temperatures (M = Fe,[1] Ru[2]) and catalytic isomerization and hydrosilation of olefins initiated at ambient temperatures by visible light irradiation[3-5] of solutions containing these cluster precursors. Interest in $M_3(CO)_{12}$ (M = Ru, Fe) complexes stems additionally from some important capabilities of trinuclear Ru and Fe carbonyl complexes,[6,7] including reduction of NO,[8] RCN,[9] and RNC[10] with H_2 on trinuclear Ru carbonyl complexes and the similar reduction of RCN on trinuclear Fe carbonyl complexes.[11] Such reactions are difficult or impossible to effect at single metal atom centers.

A major focus of our current research is to better understand and control the photochemical generation of electron deficient polynuclear metal–carbonyl complexes via dissociative ligand loss or metal framework rearrangement in an attempt to minimize cluster fragmentation[12,13] and to systematically channel reactions via associative pathways at low temperature. The $Ru_3(CO)_{12}$ and $Fe_3(CO)_{12}$ complexes serve as excellent candidates for our investigation in light of their propensity to undergo both thermal (Ru,[14] Fe[15]) and photochemical (Ru,[16] Fe[3,17]) fragmentation in fluid solution.

While relevant photoprocesses for $Ru_3(CO)_{12}$ and $Fe_3(CO)_{12}$ are not completely understood,[18-20] recent investigations of $Ru_3(CO)_{12}$ photofragmentation kinetics[21,22] have provided compelling evidence against proposals of reactive diradical intermediates and have conclusively demonstrated the existence of a reactive Ru_3 species as a primary photoproduct leading to photofragmentation. Recent flash photolysis results[23] also provide evidence for a second intermediate associated with wavelength dependent ligand photosubstitution.

Experimental Section

Instrumentation and irradiation procedures are presented in the accompanying paper in this issue.[24] Reactive gas solubilities in alkane media at 298 K and 1 atm were estimated from literature data:[25] [CO] = 0.01 M, $[C_2H_4]$ = 0.05 M, $[N_2]$ = 0.004 M.

Materials. $Fe(CO)_5$, $Fe_3(CO)_{12}$, and $Ru_3(CO)_{12}$ were obtained from Strem Chemicals. $Fe(CO)_5$ was passed through Al_2O_3 prior to use, $Fe_3(CO)_{12}$ was recrystallized from hexanes in the dark, and $Ru_3(CO)_{12}$ was used as received. $Ru(CO)_3(PPh_3)_2$, $Fe(CO)_3(PPh_3)_2$, $Ru(CO)_4(PPh_3)$, and $Fe(CO)_4(PPh_3)$ were available from previous work.[26] The PPh_3 (Aldrich) was recrystallized 3 times from EtOH. Photochemistry at 90 K was carried out by using 3-methylpentane (Aldrich, 99+%), methylcyclohexane (J.T. Baker, Photorex grade), 2-methyltetrahydrofuran (Aldrich), or 1-pentene (99+%, Phillips) as the glass material. Photochemistry at 195 K was also carried out in isooctane (J.T. Baker, Photorex grade). All solvents except 1-pentene were distilled over Na under Ar prior to use. 1-Pentene was passed through activated Al_2O_3 (neutral, Woelm) and degassed. Research grade CO, C_2H_4, and N_2 were obtained from Matheson. The ^{13}CO (99% ^{13}C, <4% ^{18}O) and $^{15}N_2$ (99% ^{15}N) were obtained from Cambridge Isotope Laboratories.

Methods. $Fe_3(CO)_{11}(PPh_3)$[27] and $Ru_3(CO)_{11}(PPh_3)$[28] complexes were prepared by literature methods. Clean solutions of $Fe(CO)_4(C_2H_4)$ and $Fe(CO)_3(C_2H_4)_2$ were prepared as previously described.[29] $Ru(CO)_5$ and $Ru(CO)_4(C_2H_4)$ were prepared quantitatively by visible light ($\lambda > 420$-nm) irradiation of 1 mM $Ru_3(CO)_{12}$ in a CO- or C_2H_4-saturated alkane solution, respectively; IR characterization of $Ru(CO)_5$[30] and $Ru(CO)_4(C_2H_4)$[16] are in accord with previous reports.

The $Ru_3(^{13}CO)_{12}$ (>95% ^{13}C) complex was prepared by near-UV irradiation of a toluene solution of $Ru_3(CO)_{12}$ under 1 atm of ^{13}CO. Removal of solvent yielded a yellow solid which was purified by chromatography on silica gel by using hexanes as eluant. The $Ru_3(^{13}CO)_n(CO)_{12-n}$ ($n \approx 5$) complex was prepared indirectly as follows. Near-UV irradiation of ~5 mM $Ru_3(CO)_{12}$ in a C_2H_4-purged isooctane solution at 298 K was discontinued after conversion to an equimolar solution of $Ru(CO)_4(C_2H_4)$ and $Ru(CO)_3(C_2H_4)_2$ as determined by IR spectroscopy.[29] Treatment of the resulting colorless solution with ^{13}CO (1 atm) at 298 K for 2 min led to rapid spectral changes without coloration of the solution, consistent with the complete conversion of $Ru(CO)_4(C_2H_4)$ and $Ru(CO)_3(C_2H_4)_2$ initially to presumed $Ru(CO)_4(^{13}CO)$ and $Ru(CO)_3(^{13}CO)_2$. The solution was then purged with Ar for 30 min to generate predominantly $Ru_3(CO)_{12-n}(^{13}CO)_n$, which was purified by chromatography (hexanes) on silica gel. Removal of solvent under vacuum yielded a yellow solid which was partially ^{13}C-enriched. Near-UV irradiation of the partially ^{13}CO-enriched $Ru_3(CO)_{12}$ in a methylcyclohexane glass at 90 K yielded loss of CO (2132 cm^{-1})[31] and ^{13}CO (2085 cm^{-1}) in a 1.5:1.0 ratio, suggesting ~40% ^{13}CO-enrichment.

Long wavelength ($\lambda > 540$-nm) irradiation of 1 mM $Fe_3(CO)_{12}$ in a C_2H_4-saturated $CF_3C_6F_{11}$ (Fluka AG) solution was monitored by ^1H

(1) (a) Manual, T. A. *J. Org. Chem.* **1962**, *27*, 3941–3945. (b) Casey, C. P.; Cyr, C. R. *J. Am. Chem. Soc.* **1973**, *95*, 2248–2253. (c) Bingham, D.; Hudson, B.; Webster, D. E.; Wells, P. B. *J. Chem. Soc., Dalton Trans.* **1974**, 1521–1524.
(2) Castiglioni, M.; Milone, L.; Osella, D.; Vaglio, G. A.; Valle, M. *Inorg. Chem.* **1976**, *15*, 394–396.
(3) Austin, R. G.; Paonessa, R. S.; Giordano, P. J.; Wrighton, M. S. *Adv. Chem. Ser.* **1978**, *68*, 189–214.
(4) Graff, J. L.; Sanner, R. D.; Wrighton, M. S. *J. Am. Chem. Soc.* **1979**, *101*, 273–275. Graff, J. L.; Sanner, R. D.; Wrighton, M. S. *Organometallics* **1982**, *1*, 837–842.
(5) Mitchener, J. C.; Wrighton, M. S. *J. Am. Chem. Soc.* **1981**, *103*, 975–977.
(6) (a) Bruce, M. I. In *Comprehensive Organometallic Chemistry*; Wilkinson, G.; Stone, F. G. A.; Abel, E. W., Eds.; Pergamon: Oxford, 1982; Vol. 4. (b) Johnson, B. F. G.; Lewis, J. *Pure App. Chem.* **1975**, *44*, 43–79. Johnson, B. F. G.; Lewis, J. *Adv. Inorg. Chem. Radiochem.* **1981**, *24*, 225–355.
(7) Deeming, A. J. In *Transition Metal Clusters*; Johnson, B. F. G., Ed.; Wiley: Chichester, 1980.
(8) Johnson, B. F. G.; Lewis, J.; Mace, J. M. *J. Chem. Soc., Chem. Commun.* **1984**, 186–188.
(9) Bernhardt, W.; Vahrenkamp, H. *Angew. Chem.* **1984**, *96*, 362–363.
(10) Bruce, M. I.; Wallis, R. C. *J. Organomet. Chem.* **1979**, *164*, C6–C8, Bruce, M. I.; Wallis, R. C. *Aust. J. Chem.* **1982**, *35*, 709–714.
(11) Andrews, M. A.; Kaesz, H. D. *J. Am. Chem. Soc.* **1977**, *99*, 6763–6765; **1979**, *101*, 7255–7259.
(12) For example, $Fe_3(CO)_{12}$ reacts with alkenes at 353 K to form $Fe(CO)_4(\eta^2$-olefin) complexes; see ref 1b.
(13) For these clusters, the average metal-metal bond energy is comparable to, not larger than, the average metal-carbon bond energy. Connor, J. A. *Top. Curr. Chem.* **1977**, *71*, 71–110.
(14) (a) Pöe, A. J.; Twigg, M. V. *Inorg. Chem.* **1974**, *13*, 2982–2985. (b) Malik, S. K.; Pöe, A. J. *Inorg. Chem.* **1978**, *17*, 1484–1488. (c) Cobbledick, R. E.; Einstein, F. W. B.; Pomeroy, R. K.; Spetch, E. R. *J. Organomet. Chem.* **1980**, *195*, 77–88.
(15) (a) Eady, C. R.; Johnson, B. F. G.; Lewis, J. *J. Chem. Soc., Dalton Trans.* **1975**, 2606–2611. (b) Clifford, A. F.; Makherjee, A. K. *Inorg. Chem.* **1963**, *2*, 151–153.
(16) Johnson, B. F. G.; Lewis, J.; Twigg, M. V. *J. Organomet. Chem.* **1974**, *67*, C75–C76, Johnson, B. F. G.; Lewis, J.; Twigg, M. V. *Dalton Trans.* **1975**, 1876–1879.
(17) Kane, V. V.; Light, J. R. C.; Whiting, M. C. *Polyhedron* **1984**, *4*, 533–538.
(18) Geoffroy, G. L.; Wrighton, M. S. *Organometallic Photochemistry*; Academic Press: New York, 1979.
(19) Tyler, D. R.; Levenson, R. A.; Gray, H. B. *J. Am. Chem. Soc.* **1978**, *100*, 7888–7893.
(20) Grevels, F.-W.; Reuvers, J. G. A.; Takats, J. *J. Am. Chem. Soc.* **1981**, *103*, 4069–4073.
(21) Desrosiers, M. F.; Ford, P. C. *Organometallics* **1982**, *1*, 1715–1716.
(22) (a) Malito, J.; Markiewicz, S.; Pöe, A. *Inorg. Chem.* **1982**, *21*, 4335–4338.
(23) (a) Desrosiers, M. F.; Wink, D. A.; Ford, P. C. *Inorg. Chem.* **1985**, *24*, 1–2. (b) Desrosiers, M. F.; Wink, D. A.; Trautman, R.; Friedman, A. E.; Ford, P. C. *J. Am. Chem. Soc.* **1986**, *108*, 1917–1927.
(24) Bentsen, J. G.; Wrighton, M. S., preceding paper in this issue.
(25) (a) Stephen, H.; Stephen, T. *Solubility of Inorganic and Organic Compounds*; Macmillan: New York, *1963*. (b) Seidel, A.; Linke, W. F. *Solubilities of Inorganic and Metal Organic Compounds*, 4th ed.; D. van Nostrand Co.; Princeton, NJ.
(26) Liu, D. K.; Brinkley, C. G.; Wrighton, M. S. *Organometallics* **1984**, *3*, 1449–1457.
(27) Bruce, M. I.; Kehoe, D. C.; Matisons, J. G.; Nicholson, B. K.; Rieger, P. H.; Williams, M. L. *J. Chem. Soc., Chem. Commun.* **1982**, 442–444.
(28) Bruce, M. I.; Matisons, J. G.; Nicholson, B. K. *J. Organomet. Chem.* **1983**, *247*, 321–343.
(29) Wuu, Y.-M.; Bentsen, J. G.; Brinkley, C. G.; Wrighton, M. S. *Inorg. Chem.* **1987**, *26*, 530–540.
(30) Rushman, P.; van Buuren, G. N.; Shirallan, M.; Pomeroy, R. K. *Organometallics* **1983**, *2*, 693–694.
(31) Leroi, G. E.; Ewing, G. E.; Pimentel, G. C. *J. Chem. Phys.* **1964**, *40*, 2298–2303.

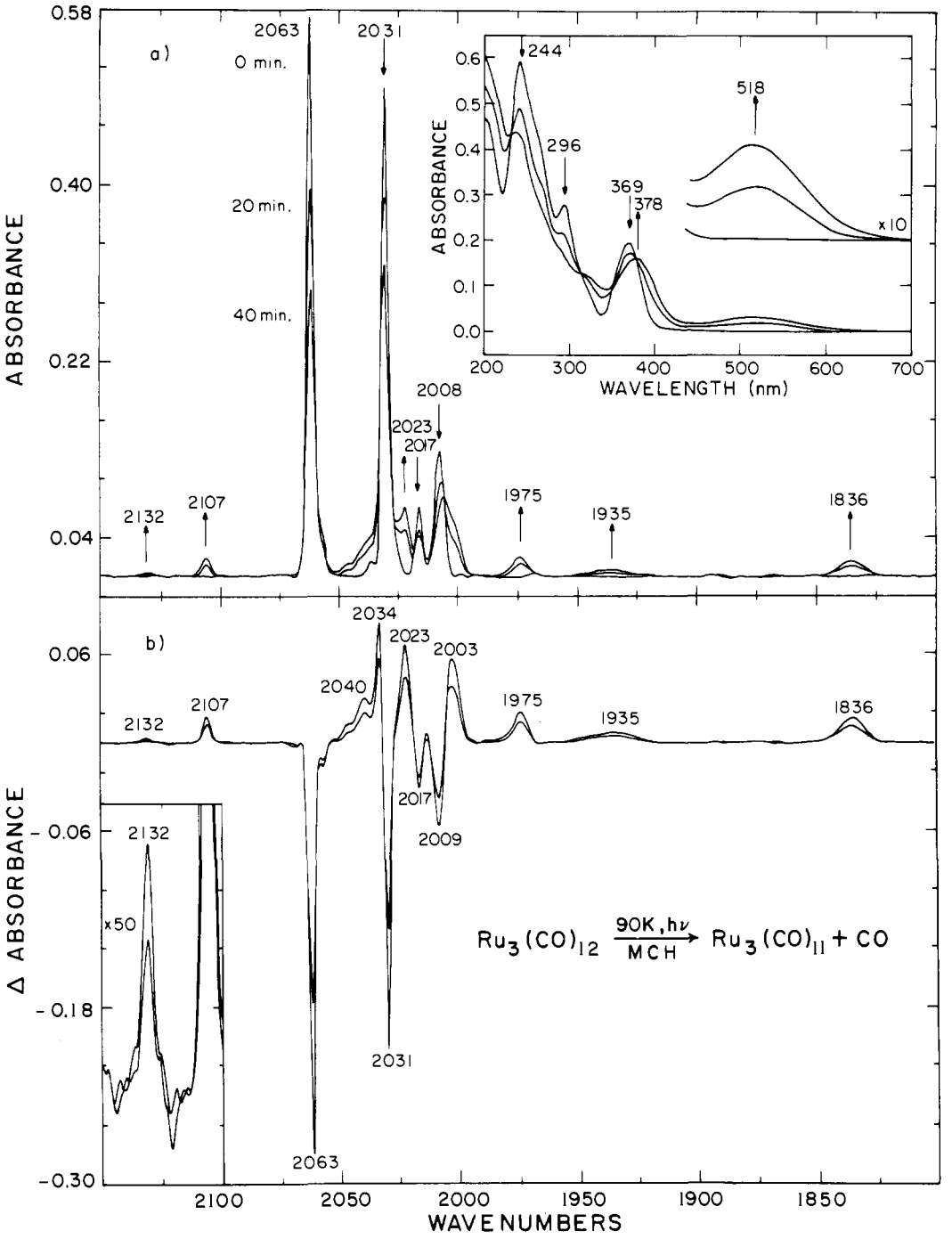

Figure 1. (a) IR and UV–vis (inset) spectral changes and (b) associated IR difference spectra accompanying near-UV irradiation of 0.1 mM $Ru_3(CO)_{12}$ in a neat MCH glass at 90 K. The $Ru_3(CO)_{12}$ solution was prepared at 298 K under Ar. The band growing in at 2132 cm^{-1} (spectrum b, inset) is attributed to free CO in the glass, while the remaining photoproduct spectral features are attributed to the bridged form of coordinatively unsaturated $Ru_3(CO)_{11}$.

NMR in a septum-sealed NMR tube. All ^1H NMR spectra were recorded on a Bruker 250-MHz Fourier transform NMR spectrometer by using cycloheptane as internal standard, 1.54 ppm vs. $SiMe_4$. The irradiation was carried out in a clear Dewar flask at 298 K by using H_2O as the thermostatic bath. Corresponding UV–vis and IR spectral changes establish the extent conversion and enable correlation of IR absorptions with integrated ^1H NMR singlets attributed to $Fe(CO)_3(C_2H_4)_2$ and $Fe(CO)_4(C_2H_4)$ products.

Results

A. Dissociative Loss of CO from $M_3(CO)_{12}$ (M = Ru, Fe) Complexes in Alkane Glasses at 90 K. (i) Characterization of CO-Bridged $Ru_3(CO)_{11}$. Broad band near-UV irradiation of ~0.1 mM $Ru_3(CO)_{12}$ in a 3-methylpentane (MP) or methylcyclohexane (MCH) glass at 90 K results in clean FTIR and UV–vis spectral changes, Figure 1, when the initial fluid solution is prepared under an Ar atmosphere. While these same spectral changes accompany 313-nm irradiation into the overlapping second and third electronic absorptions (329 sh and 296 nm, respectively), λ = 366-, 436-nm and $\lambda > 370$-nm irradiations into the low-energy tail of the first absorption band for $Ru_3(CO)_{12}$ at 90 K (centered at 369 nm) yield no spectral changes, even after prolonged irradiation. All absorbance changes in Figure 1 occur in a constant ratio at up to 90% conversion and are subsequently persistent in the dark for several hours at 90 K. The IR spectral changes show decline of absorption attributed to $Ru_3(CO)_{12}$, Table I, growth of a band at 2132 cm^{-1} associated with free CO in the glass,[31] growth of a prominent absorption at 1836 cm^{-1}, and growth of a number of bands in the region where $Ru_3(CO)_{12}$ absorbs. UV–vis spectral changes for the same sample show a decline in absorbance for the intense, metal-centered electronic transitions for $Ru_3(CO)_{12}$

Table I. IR and UV–vis Data for Relevant Complexes[a]

species	temp, K	absorption maxima: ν, cm^{-1} (ϵ or rel od)	absorption maxima: λ, nm (ϵ or rel od)
$Ru_3(CO)_{12}$	298	2061 (24 500), 2031 (14 600), 2017 (3600), 2011 (9000)	392 (7700), 322 sh (8300), 272 sh (27 000), 240 (42 000)
	90	2063 (48 000), 2031 (42 000), 2017 (6400), 2008 (12 000)	369 (17 000), 320 sh (11 000), 296 (25 000), 265 sh (39 000), 244 (53 000)
$Ru_3(CO)_{11}$ terminal form[e]	90[d]	2124 (300), 2110 (2300), 2062 (14 000), 2054 (23 000), 2042 (3400), 2033 (16 000), 2026 (20 000), 2011 (9400), 1975 (1300)	497 sh (1000), 387 (6300), 342 (10 000), 316 sh (7200), 291 (14 000), 264 sh (14 000)
$Ru_3(CO)_{11}$ bridged form[e]	90	2107 (2500), 2063 (15 000), 2039 sh (4500), 2033 (29 000), 2023 (9300), 2005 (8300), 1975 (3000), 1935 (1000), 1836 (2300)	518 (3300), 388 (14 000), 329 (8100), 273 (13 000)
	90[b]	2113 (1.0), 2075 (2.3), 2065 (6.9), 2036 (7.0), 2018 (2.6), 2008 (1.3), 1986 (1.8), 1950 (0.6), 1831 (5.8), 1824 (5.8)	
$Ru_3(CO)_{11}(N_2)$[e]	90	2248 (1400), 2108 (2900), 2059 (28 000), 2047 (25 000), 2032 (12 000), 2016 (26 000), 2004 (9800), 1986 (610)	373 (11 000), 328 sh (15 000), 297 (28 000), 269 (37 000), 244 (52 000)
$Ru_3(CO)_{11}(^{15}N_2)$[e]	90	2174 (1200), 2105 (2900), 2059 (28 000), 2047 (25 000), 2032 (12 000), 2016 (26 000), 2004 (9800), 1986 (610)	
$Ru_3(CO)_{11}(C_2H_4)$	90	2110 (1.0), 2057 (8.0), 2044 (6.0), 2024 (12), 2015 (3.4), 1999 (2.3), 1992 (1.5), 1973 (1.0)	
$Ru_3(CO)_{11}(^{13}CO)$ equil mixture	90	2063 (13), 2057 (10), 2030 (10), 2027 (8), 2017 (2), 2010 (5), 1967 (1)	
$Ru_3(CO)_{11}(^{13}CO)$ axial	90	2063 (7), 2057 (12), 2036 (3), 2027 (12), 2017 (1), 2010 (4), 1967 (1)	
$Ru_3(CO)_{11}(^{13}CO)$ equatorial[f]	90	2063 (12), 2057 (7), 2030 (15), 2017 (3), 2010 (3), 1970 (1)	
intermediate X	195[c]	2075 (1.0), 2062 (3.0), 2035 sh (1.5), 2023 (5.7), 2015 (2.2), 2010 (1.0), 1978 sh (1.0), 1970 (1.9), 1791 (1.0)	
$Ru_3(CO)_{11}$(2-MeTHF) terminal form	90[b]	2102 (1.0), 2059 (6), 2049 (11), 2026 (11), 2012 (6), 1970 (2)	
$Ru_2(CO)_8(C_2H_4)$	195[c]	2114 (0.03), 2109 (0.03), 2065 (2.2), 2030 (5.2), 2017 (3.7), 2004 (2.0), 1805 (1.0)	
$Fe_3(CO)_{12}$	298	2102 (100), 2047 (27 800), 2025 (6800), 2013 sh, 1972 (420), 1871 (340), 1840 (420)	602 (3200), 437 sh (2500), 360 sh (6400), 310 sh (14 000), 270 sh (19 000)
	90	2108 (700), 2051 (28 000), 2048 (33 000), 2029 (20 000), 2017 (4700), 2010 (5300), 1866 (1300), 1829 (3300)	605 (5200), 435 (4800), 360 sh (9200), 320 sh (19 000), 297 (20 000), 270 sh
$Fe_3(CO)_{11}$	90	2103 (200), 2059 (17 000), 2050 sh (4600), 2045 (19 000), 2035 (10 000), 2030 (6100), 2019 (8500), 2003 (1400), 1975 (1500), 1858 (1400)	
$Fe_3(CO)_{11}(C_2H_4)$	90	2096 (1.5), 2040 (4.0), 2034 (3.5), 2019 (6.5), 2001 (1.8), 1985 (2.0), 1845 (1.0), 1805 (1.6)	
	195	2095 (3), 2041 (10) 2022 (12), 2008 (6), 1815 br (1)	
$Fe_3(CO)_{11}$(2-MeTHF)	90[b]	2089 (2.0), 2031 (12), 2015 sh (8.5), 2007 (12), 1981 (3.5), 1955 (1.5), 1942 (1.8), 1835 (1.0), 1783 (1.8)	

[a] All spectra are measured in methylcyclohexane unless specified otherwise; IR spectra are recorded at 2-cm^{-1} resolution and UV–vis data are accurate to ±2 nm. Extinction coefficients are uncorrected for solvent contraction. [b] In 2-MeTHF. [c] In isooctane. [d] In a methylcyclohexane glass doped with 1% 3-methylpentane. [e] Extinction coefficients estimated assuming clean conversion to a single product by digital subtraction of spectral features associated with unreacted $M_3(CO)_{12}$. [f] Relative intensities estimated by digital subtraction of the 90 K spectral features for axial-^{13}CO–$Ru_3(CO)_{11}(^{13}CO)$ from those obtained at 90 K for the equilibrium mixture of isoenergetic isomers.

at 369 and 296 nm, concomitant growth of equally intense electronic absorbances at 388 and 329 nm (sh), maintenance of an isobestic point at 378 nm, and growth of a weak, low-energy absorption centered at 518 nm. The 2132-cm^{-1} feature shows that dissociative loss of CO occurs from photoexcited $Ru_3(CO)_{12}$. In accord with a previous report,[32] the molar absorptivity of free CO (~400 M^{-1} cm^{-1} at 2132 cm^{-1}) in a 90 K MCH glass has been determined independently by measuring the absorptivity at 2132 cm^{-1} for known fractional light-induced conversion of $Cr(CO)_6$ or $W(CO)_6$ to CO and the appropriate $M(CO)_5$ fragment. This result allows quantitative determination of the number of CO molecules liberated in the photolysis of $Ru_3(CO)_{12}$ at 90 K. Determination of the stoichiometry of CO loss from photoexcited $Ru_3(CO)_{12}$ in MCH at 90 K is complicated by the fact that, in Figure 1, direct quantitation of the photochemical consumption of $Ru_3(CO)_{12}$ is not possible due to overlapping reactant and product electronic and IR absorption features. In particular, both $Ru_3(CO)_{12}$ and the CO-bridged photoproduct absorb strongly at 2063 cm^{-1}. To alleviate this problem, the observed photoproduct is reacted with excess L = N_2 or C_2H_4 at low temperature to yield $Ru_3(CO)_{11}L$ complexes which do not absorb at 2063 cm^{-1}; the amount of free CO in the glasses does not change during these reactions. Importantly, the amount of free CO detected is consistent with the loss of *one* CO per molecule of $Ru_3(CO)_{12}$ consumed in the initial photolysis, even at >90% conversion. For the observed photoproduct, the 518-nm feature is consistent with coordinative unsaturation; the 388- and 329-nm features suggest retention of the trinuclear cluster framework, and the 1836 cm^{-1} feature indicates a structure containing at least one bridging CO ligand. Thus, eq 1 represents the low-temperature photochemistry of $Ru_3(CO)_{12}$ in an alkane glass. Consistent with its formulation, photogenerated $Ru_3(CO)_{11}$ reacts upon warmup with PPh_3 (vide infra) to yield $Ru_3(CO)_{11}(PPh_3)$.

The 1836-cm^{-1} feature for the bridged form of $Ru_3(CO)_{11}$ is replaced by a 1794-cm^{-1} absorbance when $Ru_3(^{13}CO)_{12}$ is irradiated in place of $Ru_3(CO)_{12}$ at 90 K. During photolysis the 2085-cm^{-1} (photoejected ^{13}CO) and 1794-cm^{-1} ($Ru_3(^{13}CO)_{11}$) features grow in the same constant ratio observed for the 2132- and 1836-cm^{-1} features associated with irradiation of natural abundance $Ru_3(CO)_{12}$. When $Ru_3(CO)_{12-n}(^{13}CO)_n$ is irradiated at 90 K, the free ^{12}CO (2132-cm^{-1}) and ^{13}CO (2085-cm^{-1}) features grow in a 1.5:1 ratio, and prominent bridging carbonyl features, attributed to photogenerated $Ru_3(CO)_{11-m}(^{13}CO)_m$, grow in a 1.5:1 ratio at 1836 and 1794 cm^{-1}, consistent with ~40% ^{13}C-enrichment. Importantly, an additional shoulder is observed at 1805 cm^{-1}. The band shapes observed in the bridging CO region for $Ru_3(CO)_{11-m}(^{13}CO)_m$ do not conform to a superposition of bridging

(32) Pope, K. R.; Wrighton, M. S. *Inorg. Chem.* **1985**, *24*, 2792–2796.

spectral features observed for $Ru_3(CO)_{11}$ and $Ru_3(^{13}CO)_{11}$. While not conclusive, these results suggest vibrational coupling of multiple bridging CO oscillators for $Ru_3(CO)_{11}$. Furthermore, IR spectral data support a similar CO-bridged structure for $Ru_3(CO)_{11}$ in a 2-methyltetrahydrofuran (2-MeTHF) glass at 90 K (vide infra). In this glass the CO-bridging feature shifts to lower energy and is split into two distinct absorbances at 1831 and 1824 cm^{-1}. Similar medium dependent spectral shifts are observed in the bridging CO region for $Fe_3(CO)_{12}$ and for *trans*-$(\eta^5$-$C_5Me_5)_2Fe_2(CO)_4$[33] at 90 K.

(ii) Characterization of CO-Bridged $Fe_3(CO)_{11}$. In an alkane glass at 90 K the IR spectral features for $Fe_3(CO)_{12}$ are in close agreement with those reported previously[34] in Ar and N_2 matrices at 20 K, consistent with site-separated $Fe_3(CO)_{12}$ molecules having the doubly bridged C_{2v} structure observed in the solid state,[35] Table I. The 90 K spectra are complicated by aggregation at concentrations of $Fe_3(CO)_{12}$ exceeding 0.02 mM. This low concentration of $Fe_3(CO)_{12}$ needed to circumvent aggregation has severely limited low-temperature investigations of this complex. The UV–vis spectrum at 90 K shows features similar to those observed for the terminal form in fluid solution at 298 K. As previously noted,[19] the first electronic absorption for $Fe_3(CO)_{12}$ red-shifts slightly on cooling, while the second electronic absorption blue-shifts. Both features are well-resolved from higher energy features at 90 K, thus enabling selective excitation with $\lambda > 540$-nm or $\lambda = 436$-nm irradiation, respectively.

Near-UV irradiation of ~0.02 mM $Fe_3(CO)_{12}$ in a MCH glass at 90 K yields clean FTIR and UV–vis spectral changes which occur in constant ratio at up to 90% conversion and persist for several hours at 90 K. While these same spectral changes accompany 313 and 366-nm irradiation into the third electronic absorption, 436-nm photoconversion proceeds extremely slowly and $\lambda > 540$-nm irradiation into the first absorption band for $Fe_3(CO)_{12}$ at 90 K (centered at 605 nm) yields no spectral changes, even after prolonged irradiation. When photoconversion is achieved, the decline of IR absorptions for $Fe_3(CO)_{12}$ is accompanied by growth of absorption at 2132 cm^{-1}, growth of a prominent absorption at 1858 cm^{-1}, and growth of new terminal CO features in the region of those for $Fe_3(CO)_{12}$. Corresponding UV–vis spectral changes show a decline in the absorbance for the intense metal-centered electronic transitions associated with $Fe_3(CO)_{12}$ at 605 and 435 nm and corresponding growth of intense overlapping featureless absorption which tails to wavelengths longer than 800 nm. The magnitude of 2132-cm^{-1} absorption shows loss of one CO molecule per $Fe_3(CO)_{12}$ consumed, and the electronic spectral changes suggest retention of Fe–Fe bonding interactions in the product. Importantly, IR spectral features for the Fe photoproduct are similar to those obtained for the bridged form of $Ru_3(CO)_{11}$, suggesting a similar structure for photogenerated $Fe_3(CO)_{11}$, Table I. Interestingly, the corresponding $Os_3(CO)_{11}$ complex has no bridging CO's.[24]

(iii) Reaction of Photogenerated $M_3(CO)_{11}$ (M = Ru, Fe) Complexes with PPh_3. Warmup to 298 K of a 90 K MCH glass containing photoejected CO and the accumulated CO-bridged forms of $M_3(CO)_{11}$ (M = Ru, Fe) results in quantitative regeneration of $M_3(CO)_{12}$. For Ru, similar warmup to 298 K in the presence of 10 mM PPh_3 or 10 mM PPh_3 and 10 mM CCl_4 yields net IR spectral changes at 298 K consistent with regeneration of $Ru_3(CO)_{12}$ in competition with quantitative conversion of irreversibly consumed $Ru_3(CO)_{12}$ to the well-characterized $Ru_3(CO)_{11}(PPh_3)$ complex.[36] For Fe, warmup to 195 K in the presence of 10 mM PPh_3 yields $Fe_3(CO)_{11}(PPh_3)$. In accord with the known thermal lability of $Fe_3(CO)_{11}(PPh_3)$,[37] further warmup to 298 K of this 195 K solution results in fragmentation of the $Fe_3(CO)_{11}(PPh_3)$ complex to give a mixture of $Fe(CO)_4(PPh_3)$ and $Fe(CO)_3(PPh_3)_2$ complexes. Mononuclear $M(CO)_4(PPh_3)$ and $M(CO)_3(PPh_3)_2$ complexes are not obtained for M = Ru at 298 K or for M = Fe at 195 K, consistent with light-induced loss of CO from $M_3(CO)_{12}$ at 90 K according to eq 1. Photofragmentation of the M_3 framework of $M_3(CO)_{12}$ at 90 K apparently does not occur. Also, thermal reaction of $M_3(CO)_{11}$ with PPh_3 does not lead to fragmentation.

Interestingly, warmup to 298 K of 90 K MCH glasses containing photogenerated $Ru_3(CO)_{11}$ (0.05 mM), photoejected CO, and 2 mM or 10 mM PPh_3 gives 50% and 30% regeneration of $Ru_3(CO)_{12}$, respectively. These results suggest a significant selectivity for reaction of $Ru_3(CO)_{11}$ with CO vs. PPh_3, consistent with a delocalized unsaturation in $Ru_3(CO)_{11}$.

(iv) Reaction of $M_3(CO)_{11}$ (M = Ru, Fe) Complexes with $2e^-$ Donor Ligands at Low Temperature. For 90 K MP or MCH glasses containing photogenerated $M_3(CO)_{11}$ (bridged form, M = Ru, Fe) and similar concentrations of deliberately added excess CO, the rate of regeneration of $M_3(CO)_{12}$ is orders of magnitude greater in MP than in MCH. At 90 K, the $M_3(CO)_{11}$ species react to regenerate $M_3(CO)_{12}$ in MP, but in MCH $M_3(CO)_{11}$ is inert. However, warming the MCH glass to 110 K retains the integrity of the glass and results in rapid IR spectral changes which persist on recooling the glass to 90 K, consistent with quantitative regeneration of $M_3(CO)_{12}$. In the absence of excess CO, the bridged forms of $Ru_3(CO)_{11}$ and $Fe_3(CO)_{11}$ persist undiminished during a similar excursion to 110 K in MCH. As in studies of $Os_3(CO)_{11}$,[24] such kinetic control has enabled leisurely investigation of the bimolecular reactions of photogenerated $Ru_3(CO)_{11}$ with CO, N_2, and C_2H_4 according to eq 3.

$$Ru_3(CO)_{11} + L \xrightarrow[L = CO,\ N_2,\ C_2H_4]{110\ K,\ alkane} Ru_3(CO)_{11}L \qquad (3)$$

Preparation of $Ru_3(CO)_{11}(N_2)$. Data in Figure 2 establishes reaction of $Ru_3(CO)_{11}$ with N_2 to give $Ru_3(CO)_{11}(N_2)$. Near-UV irradiation of ~0.1 mM $Ru_3(CO)_{12}$ in a N_2-containing MCH glass at 90 K results in initial IR and UV–vis spectral changes consistent with Figure 1 and eq 1. Warmup to 110 K of the irradiated 90 K glass yields IR and UV–vis spectral changes which persist on recooling the glass to 90 K. Figure 2a shows the net IR spectral changes associated only with the 110 K excursion. Negative deviations indicate decline of the CO-bridged form of photogenerated $Ru_3(CO)_{11}$, while positive deviations are associated with formation of $Ru_3(CO)_{11}(N_2)$. Complete decline of the 518-nm and 1836-cm^{-1} features during the 110 K excursion indicates quantitative consumption of CO-bridged $Ru_3(CO)_{11}$ by reaction with N_2 to yield $Ru_3(CO)_{11}(N_2)$, exhibiting only terminal CO features similar to those for axially (perpendicular to the plane defined by the trinuclear M_3 framework) substituted $Os_3(CO)_{11}(N_2)$.[24] An associated feature at 2248 cm^{-1} (Figure 2a, insert) is attributed to coordinated N_2 and shifts to 2174 cm^{-1} (predicted at 2172 cm^{-1}) when $^{15}N_2$ (99% ^{15}N) is used as the reagent gas (Figure 2b). Bound N_2 induces a secondary isotope shift of three wavenumbers for the product CO feature which overlaps the declining 2107-cm^{-1} feature of the bridged form of $Ru_3(CO)_{11}$. Repetition of this experiment using a 50:50 mixture of $^{15}N_2$ and $^{14}N_2$ gives net FTIR spectral changes which resemble a superposition of the spectral features presented in Figure 2 (parts a and b) for reaction of $Ru_3(CO)_{11}$ with the isotopically pure gases. The absence of a weak low-energy (~500 nm) electronic absorption feature in $Ru_3(CO)_{11}(N_2)$ is consistent with the fact that the N_2 adduct is coordinatively saturated. $Ru_3(CO)_{11}(N_2)$ has an electronic absorption spectrum (Table I) that is very similar to that found in the near-UV for $Ru_3(CO)_{12}$, indicating retention of a relatively unperturbed Ru_3 framework upon conversion of $Ru_3(CO)_{12}$ to $Ru_3(CO)_{11}(N_2)$.

The absence of any absorbance change at 2132 cm^{-1} for the 110 K excursion (Figure 2, insets) indicates that the amount of photogenerated CO remains constant in the glass upon conversion of the initial CO-bridged photoproduct to $Ru_3(CO)_{11}(N_2)$. Since $Ru_3(CO)_{12}$ is thermally inert at 110 K, the negative deviations at 2063 and 2033 cm^{-1} in Figure 2 (parts a and b) can only be

(33) Hepp, A. H.; Blaha, J. P.; Lewis, C.; Wrighton, M. S. *Organometallics* **1984**, *3*, 174–177.
(34) Poliakoff, M.; Turner, J. J. *J. Chem. Soc. A* **1971**, 654–658.
(35) (a) Wei, C. H.; Dahl, L. F. *J. Am. Chem. Soc.* **1969**, *91*, 1351–1361. (b) Cotton, F. A.; Troup, J. M. *J. Am. Chem. Soc.* **1974**, *96*, 4155–4159.
(36) Forbes, E. J.; Goodhand, N.; Jones, D. L. *J. Organomet. Chem.* **1979**, *182*, 143–154.
(37) Angelici, R. J.; Siefert, E. E. *Inorg. Chem.* **1966**, *5*, 1457–1459.

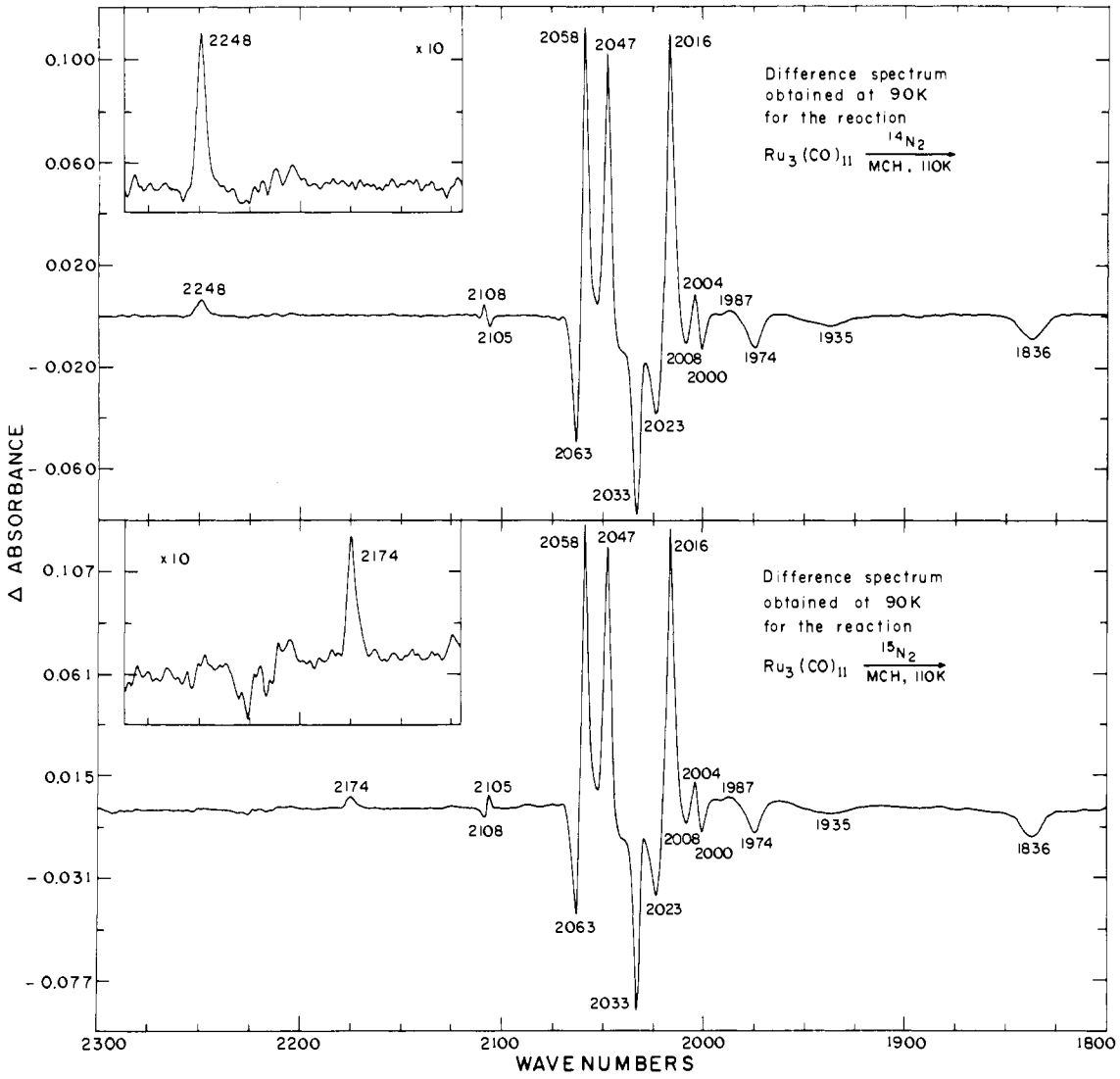

Figure 2. IR difference spectral changes at 90 K associated with brief warming to 110 K of a 90 K MCH glass containing photogenerated $Ru_3(CO)_{11}$, photoejected CO, unreacted $Ru_3(CO)_{12}$, and excess N_2. Negative deviations are associated with consumption of the bridged form of photogenerated $Ru_3(CO)_{11}$, while positive deviations are associated with conversion to $Ru_3(CO)_{11}(N_2)$. The band growing in at 2248 cm^{-1} (inset) is assigned as a coordinated N_2 stretch. (b) Corresponding IR difference spectral changes for reaction of photogenerated $Ru_3(CO)_{11}$ (bridged form) with $^{15}N_2$; the band growing in at 2174 cm^{-1} (inset) is assigned as a coordinated $^{15}N_2$ stretch.

attributed to the decline of $Ru_3(CO)_{11}$ absorption features which overlap those for $Ru_3(CO)_{12}$. Establishment of the relative absorptivities of $Ru_3(CO)_{12}$ and bridged $Ru_3(CO)_{11}$ at 2063 and 2033 cm^{-1} enables a clean stoichiometric determination in Figure 1 of *one* photoejected CO per $Ru_3(CO)_{12}$ molecule consumed and allows deconvolution of the remaining spectral features for the CO-bridged $Ru_3(CO)_{11}$. Importantly, absorbance changes associated with the two-step conversion of $Ru_3(CO)_{12}$ to $Ru_3(CO)_{11}(N_2)$ are consistent with the presence of one free CO (2132 cm^{-1}) for every $Ru_3(CO)_{12}$ (2063 cm^{-1}) consumed to form $Ru_3(CO)_{11}(N_2)$ (see Supplementary Material). This result supports the formulation of $Ru_3(CO)_{11}$ as a species derived from the loss of *one* CO from $Ru_3(CO)_{12}$.

Not surprisingly, the N_2 of $Ru_3(CO)_{11}(N_2)$ is readily liberated and replaced by $2e^-$ donors. Warmup to 195 K of a 90 K alkane glass containing photogenerated $Ru_3(CO)_{11}(N_2)$, photoejected CO, and excess N_2 leads to quantitative regeneration of $Ru_3(CO)_{12}$, while warmup to 298 K in the presence of 10 mM PPh_3 yields $Ru_3(CO)_{11}(PPh_3)$, competitive with $Ru_3(CO)_{12}$ regeneration.

Preparation of $M_3(CO)_{11}(\eta^2$-alkene) Complexes (M = Ru, Fe). In strict analogy to the preparation of $Ru_3(CO)_{11}(N_2)$, warmup to 110 K of a MCH glass containing photogenerated $M_3(CO)_{11}$ (M = Ru, Fe), photoejected CO, and excess C_2H_4 (<10 mM) yields FTIR characterized products formulated as $M_3(CO)_{11}(C_2H_4)$, Table I. $Ru_3(CO)_{11}(C_2H_4)$ exhibits only terminal carbonyl features analogous to those reported previously for the well characterized, equatorially substituted $Os_3(CO)_{11}(C_2H_4)$ complex.[38] The net spectral changes associated with the two-step conversion of $Ru_3(CO)_{12}$ to $Ru_3(CO)_{11}(C_2H_4)$ at low temperature are again consistent with initial photoejection of one CO from $Ru_3(CO)_{12}$. $Fe_3(CO)_{11}(C_2H_4)$ exhibits bridging CO features at 1845 and 1805 cm^{-1}, suggesting a structure related to the C_{2v} isomer of $Fe_3(CO)_{12}$ by replacement of C_2H_4 for a terminal CO. Slow, but complete, regeneration of the terminal form of $Fe_3(CO)_{12}$ accompanies warmup of $Fe_3(CO)_{11}(C_2H_4)$ and free CO to 195 K. The $M_3(CO)_{11}(C_2H_4)$ (M = Ru, Fe) complexes are more labile than the well-characterized $Os_3(CO)_{11}(C_2H_4)$ complex and have thus far eluded ^1H NMR characterization in fluid solutions at 195 K.

Near-UV irradiation of ~0.1 mM $Ru_3(CO)_{12}$ or ~0.02 mM $Fe_3(CO)_{12}$ in neat 1-pentene glasses at 90 K initially yields decline of IR spectral features for $M_3(CO)_{12}$, growth of absorption at 2132 cm^{-1} in an amount consistent with the loss of one CO, and growth of new CO features closely related to those observed in alkane glasses for $M_3(CO)_{11}(C_2H_4)$ (M = Ru, Fe). These new spectral features are consistent with direct photogeneration of M_3-

(38) Johnson, B. F. G.; Lewis, J.; Pippard, D. A. *J. Chem. Soc., Dalton Trans.* **1981**, 407–412.

$(CO)_{11}(\eta^2\text{-}C_5H_{10})$ complexes. Continued irradiation yields unidentified secondary photoproducts after >50% conversion of the starting clusters.

Preparation of Axial-^{13}CO–$Ru_3(CO)_{11}(^{13}CO)$. IR spectral data presented as Supplementary Material confirm that photogenerated, CO-bridged $Ru_3(CO)_{11}$ reacts with ^{13}CO in a kinetically controlled fashion to yield axial-^{13}CO–$Ru_3(CO)_{11}(^{13}CO)$ under conditions where fluxional processes associated with interconversion of the isoenergetic axial- and equatorial-^{13}CO–$Ru_3(CO)_{11}(^{13}CO)$ complexes are completely suppressed. Near-UV irradiation of ~0.1 mM $Ru_3(CO)_{12}$ in a ^{13}CO-containing (~1 mM as judged by FTIR absorbance at 2085 cm^{-1}) MCH glass at 90 K yields IR and UV–vis spectral changes consistent with clean photogeneration of free ^{12}CO (2132 cm^{-1}) and the bridged form of $Ru_3(CO)_{11}$ (1836 cm^{-1}) according to eq 1. Warmup of this irradiated 90 K glass to 110 K gives IR spectral changes which persist on recooling the glass to 90 K. Complete restoration of all UV–vis spectral features to coincidence with those initially present for $Ru_3(CO)_{12}$ suggests that only $Ru_3(CO)_{11}(^{13}CO)$ is formed. Subsequent warmup of this 90 K glass to 298 K yields new IR spectral changes which persist on recooling the sample to 90 K. The 90 K UV–vis spectrum is unaltered by this excursion to 298 K, indicating complete retention of $Ru_3(CO)_{11}(^{13}CO)$ and $Ru_3(CO)_{12}$ species. The IR spectral features associated with $Ru_3(CO)_{11}(^{13}CO)$ clearly change as a result of the 298 K excursion, consistent with the original formation of a nonequilibrium excess of one isomer of $Ru_3(CO)_{11}(^{13}CO)$ during the initial 110 K excursion. Previous ^{13}C NMR investigations for $Ru_3(CO)_{12}$[39] indicate that complete equilibration to an equal mixture of two $Ru_3(CO)_{11}(^{13}CO)$ isomers should be rapid on the time scale of the 298 K excursion. Indeed, the final IR spectral features are in close agreement with those reported previously[40] for the mixture of $Ru_3(CO)_{11}(^{13}CO)$ isomers in alkane media at 298 K. The 50% (±4%) decline of an intense 2027-cm^{-1} product feature as a result of the 298 K excursion establishes that only one isomer of $Ru_3(CO)_{11}(^{13}CO)$ is obtained in the initial 110 K excursion. These IR spectral changes for Ru are similar to those established to result from conversion of isomerically pure axial-^{13}CO–$Os_3(CO)_{11}(^{13}CO)$ to an equal mixture of axial- and equatorial-^{13}CO isomers under similar conditions.[24] The 90 K IR spectral features for each of the two $Ru_3(CO)_{11}(^{13}CO)$ isomers have been deconvoluted, Table I, and absolute configurations assigned on the basis of considerations applied to the Os case, thereby establishing the conversion of the bridged form of $Ru_3(CO)_{11}$ cleanly to axial-^{13}CO–$Ru_3(CO)_{11}(^{13}CO)$ at low temperature. The spectral features obtained here for the two isomers of $Ru_3(CO)_{11}(^{13}CO)$ are in excellent agreement with those derived by Battiston et al.[40] This finding is consistent with an axial vacancy in the CO-bridged $Ru_3(CO)_{11}$ fragment. Interestingly, near-UV irradiation of axial-^{13}CO–$Ru_3(CO)_{11}(^{13}CO)$ at 90 K yields IR spectral changes consistent with scrambling of the $Ru_3(CO)_{11}(^{13}CO)$ isomers on a time scale which is rapid compared to CO loss. Detailed studies of ^{13}CO reaction with $Fe_3(CO)_{11}$ were not carried out due to the difficulties encountered with low concentrations of $Fe_3(CO)_{12}$.

(v) Isomerization of $Ru_3(CO)_{11}$ from a Terminal Form to a CO-Bridged Form. While $Ru_3(CO)_{11}$ and $Fe_3(CO)_{11}$ preferentially adopt a CO-bridged structure in alkane glasses at 90 K, $Os_3(CO)_{11}$ adopts an all terminal axially vacant structure.[24] Interestingly, in a neat MCH glass at 90 K, the axially vacant terminal form of $Ru_3(CO)_{11}$ is detected by rapid scan FTIR subsequent to a flash irradiation of the sample, but IR features for this initial product decline within 30 s to yield the persistent spectral features illustrated in Figure 1 for accumulation of the CO-bridged form of $Ru_3(CO)_{11}$. However, subtle factors control whether the terminal or bridged form of $Ru_3(CO)_{11}$ will be accumulated from irradiation of $Ru_3(CO)_{12}$ at 90 K.

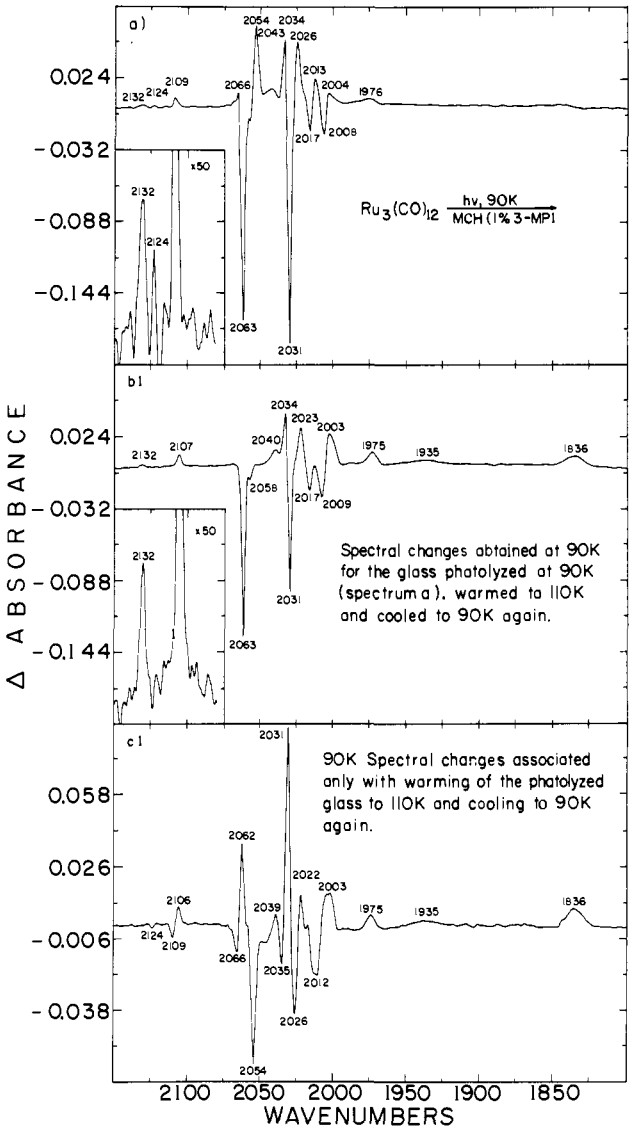

Figure 3. (a) IR difference spectral changes accompanying near-UV irradiation of 0.1 mM $Ru_3(CO)_{12}$ in a 90 K MCH glass doped with 1% MP. The $Ru_3(CO)_{12}$ solution was prepared under Ar. The band growing in at 2132 cm^{-1} (inset) is attributed to free CO in the glass, while the remaining photoproduct spectral features are attributed to the terminal form of coordinatively unsaturated $Ru_3(CO)_{11}$. (b) IR difference spectral changes were obtained at 90 K for the glass photolyzed at 90 K (spectrum a), warmed to ~110 K, and recooled to 90 K again. The negative absorbance changes are associated with consumption of $Ru_3(CO)_{12}$ during the initial photolysis; the positive absorbance changes are attributed to the bridged form of $Ru_3(CO)_{11}$, obtained by isomerization from the terminal form of photogenerated $Ru_3(CO)_{11}$. The band associated with free CO at 2132 cm^{-1} (inset) remains unchanged during the 110 K excursion. (c) IR difference spectral changes at 90 K associated only with the 110 K excursion (difference between spectra a and b). Negative deviations are associated with decline of the terminal form of photogenerated $Ru_3(CO)_{11}$ while positive deviations are associated with conversion to the bridged form of $Ru_3(CO)_{11}$.

Near-UV irradiation of ~0.1 mM $Ru_3(CO)_{12}$ in a MP doped (1%) MCH glass at 90 K yields persistent FTIR and UV–vis spectral changes, Figure 3a, significantly different from those which persist in the pure MCH glass, Figure 1. The IR spectral changes in Figure 3a show decline of absorption features for $Ru_3(CO)_{12}$, growth of a band at 2132 cm^{-1} associated with free CO, and growth of a new set of terminal carbonyl features, some of which overlap those for $Ru_3(CO)_{12}$. Conspicuously absent is the bridging CO feature diagnostic for the bridged form of $Ru_3(CO)_{11}$. Associated UV–vis spectral changes (not shown) show

(39) (a) Forster, A.; Johnson, B. F. G.; Lewis, J.; Matheson, T. W.; Robinson, B. H.; Jackson, W. G. *J. Chem. Soc., Chem. Commun.* **1974**, 1042–1044. (b) Milone, L.; Aime, S.; Randall, E. W.; Rosenberg, E. *J. Chem. Soc., Chem. Commun.* **1975**, 452–454. (c) Johnson, B. F. G.; Lewis, J.; Reichert, B. E.; Schorpp, K. T. *J. Chem. Soc., Dalton Trans.* **1976**, 1403–1404.

(40) Battiston, G. A.; Bor, G.; Dietter, U. K.; Kettle, S. F. A.; Rossetti, R.; Sbrignaddelo, G.; Stanghellini, P. L. *Inorg. Chem.* **1980**, *19*, 1961–1973.

a decline in absorbance for the intense 369- and 296-nm features of $Ru_3(CO)_{12}$, growth of equally intense electronic absorptions at 387 and 342 nm, and growth of a weak, low-energy absorption shoulder at 497 nm. Warmup to 110 K of the irradiated 90 K glass yields IR and UV–vis spectral changes which persist on recooling the glass to 90 K, Figure 3 (parts b and c) (IR changes only). The IR spectral changes in Figure 3b are consistent with quantitative conversion of irreversibly consumed $Ru_3(CO)_{12}$ (negative deviations) to the CO-bridged form of $Ru_3(CO)_{11}$ [ν (cm^{-1}) = 1836; λ (nm) = 518] (positive deviations). The IR spectral features in Figure 3c are consistent with complete conversion of the primary photoproduct (negative deviations) to the CO-bridged $Ru_3(CO)_{11}$ (positive deviations), without significant regeneration of $Ru_3(CO)_{12}$. Positive deviations at 2063 and 2033 cm^{-1} (Figure 3c) are attributed to the bridged form of $Ru_3(CO)_{11}$. A second excursion to 110 K yields no further spectral changes. Importantly, comparison of the 90 K absorbance changes in the insets of Figure 3 (parts a and b) shows that the amount of free CO (2132 cm^{-1}) detected in the glass remains unchanged during conversion at 110 K of the initial photoproduct to the bridged form of $Ru_3(CO)_{11}$. For the initial photoproduct, the low-energy 497-nm feature is consistent with coordinative unsaturation, and the 387- and 342-nm features suggest retention of the trinuclear cluster framework. IR spectral features for the initial photoproduct are similar to those for the well established axially vacant $Os_3(CO)_{11}$ complex.[24] These results suggest formulation of the initial photoproduct (responsible for the persistent product features in Figure 3a) as an axially vacant form of $Ru_3(CO)_{11}$ with only terminal CO's. The axially vacant $Os_3(CO)_{11}$ complex reacts with ^{13}CO at low temperature to yield axial-^{13}CO–$Os_3(CO)_{11}(^{13}CO)$.[24] Similar reaction chemistry is obtained for the CO-bridged isomer of $Ru_3(CO)_{11}$, establishing that an axial vacancy is preserved in the isomerization of $Ru_3(CO)_{11}$ from the all terminal form (adopted by $Os_3(CO)_{11}$) to the CO-bridged form (adopted by $Fe_3(CO)_{11}$). As discussed for Os,[24] electronic factors favor an axial vacancy trans to CO, rather than an equatorial vacancy, trans to a metal–metal bond, in photogenerated $M_3(CO)_{11}$ (M = Fe, Ru, Os). The structure of CO-bridged $M_3(CO)_{11}$ (M = Ru, Fe) cannot be determined with certainty from the available IR data. The weak, low-energy, visible absorption associated with the axial vacancy in the two detected isomers of $Ru_3(CO)_{11}$ can be attributed to the appearance of a low-lying acceptor orbital of predominantly d_{z^2} parentage, which becomes the new LUMO.[41,42]

(vi) Irradiation of $Ru_3(CO)_{12}$ and $Fe_3(CO)_{12}$ in a 2-Methyltetrahydrofuran Glass at 90 K. $Ru_3(CO)_{12}$. Near-UV irradiation of ~0.1 mM $Ru_3(CO)_{12}$ in a 90 K 2-MeTHF glass results in rapid IR and UV–vis spectral changes, and secondary photoproduct formation complicates the spectra at low extents (<5%) of photochemical conversion. At <2% conversion, IR spectral changes show decline of absorption for $Ru_3(CO)_{12}$, growth of absorption at 2132 cm^{-1} associated with free CO in the glass, and growth of a number of terminal CO features in the region where $Ru_3(CO)_{12}$ absorbs. Corresponding UV–vis spectral changes show a decline in absorbance for the intense metal-centered electronic transitions of $Ru_3(CO)_{12}$ at 369 and 295 nm and concomitant growth of an equally intense feature which is red-shifted from the 369-nm feature and tails to wavelengths as long as 500 nm. Within experimental error, the amount of free CO detected at 2132 cm^{-1} is consistent with the appearance of one CO for every $Ru_3(CO)_{12}$ consumed ($\epsilon_{CO} \approx 350\ M^{-1}\ cm^{-1}$ in 2-MeTHF at 90 K).[32] Electronic spectral features suggest retention of the Ru_3 framework in the initial product. IR and UV–vis spectral changes observed for the photolysis of $Ru_3(CO)_{12}$ in 2-MeTHF at 90 K are very similar to those observed for the conversion of $Ru_3(CO)_{12}$ to $Ru_3(CO)_{11}(P(OMe)_3)$ in alkane solution at 298 K.[23] On the basis of this characterization and reaction chemistry described below, the initially observed photoproduct in 2-MeTHF at 90 K is formulated as $Ru_3(CO)_{11}$(2-MeTHF) with only terminal CO's, Table I.

Warmup to 110 K of the irradiated 90 K glass containing $Ru_3(CO)_{11}$(2-MeTHF) yields rapid IR and UV–vis spectral changes which persist on recooling the glass to 90 K; these same spectral changes occur slowly ($t_{1/2} \approx 1$ h) in the dark at 90 K. The IR spectral changes show complete decline of absorptions attributed to the terminal form of $Ru_3(CO)_{11}$(2-MeTHF), growth of a prominent bridging absorption (1831, 1824 cm^{-1}), and growth of a new set of terminal carbonyl features in the region where $Ru_3(CO)_{12}$ absorbs. Regeneration of $Ru_3(CO)_{12}$ is not detected. Corresponding UV–vis spectral changes correlate growth of the bridging CO feature with growth of an intense electronic absorption feature at 380 nm. Importantly, the amount of photoejected CO (2132 cm^{-1}) remains unchanged during the 110 K excursion, consistent with retention of 11 CO's in the new product. The bridging CO features suggest more than one ketonic or semibridging CO, while the electronic spectral features suggest retention of the Ru_3 framework in the new product. The IR spectral features suggest a similar structure for the CO-bridged product in 2-MeTHF and for $Ru_3(CO)_{11}$ in MCH, but the bridging CO feature shifts to lower energy in 2-MeTHF. We tentatively formulate the CO-bridged product in 2-MeTHF as coordinatively unsaturated $Ru_3(CO)_{11}$, Table I, which is structurally related to CO-bridged $Ru_3(CO)_{11}$ in MCH. Due to the small sample thickness (2-MeTHF is less transparent than MCH in the CO stretching region, where reaction progress is conveniently monitored) and low extents of photochemical conversion in 2-MeTHF vs. MCH, a weak, low-energy, electronic transition for $Ru_3(CO)_{11}$ in 2-MeTHF would go undetected unless it were considerably more intense than the 518-nm feature observed for $Ru_3(CO)_{11}$ in MCH. Since no such feature is detected in 2-MeTHF, we cannot rule out the possible coordination of solvent and formulation of the CO-bridged product in 2-MeTHF as a bridged form of coordinatively saturated $Ru_3(CO)_{11}$(2-MeTHF).

Brief (30 s) near-UV irradiation of the 90 K 2-MeTHF glass containing photoejected CO, CO-bridged $Ru_3(CO)_{11}$, and unreacted $Ru_3(CO)_{12}$ yields IR spectral changes consistent with additional conversion (2%) of more $Ru_3(CO)_{12}$ to the terminal form of $Ru_3(CO)_{11}$(2-MeTHF), without change in the spectral features for the CO-bridged $Ru_3(CO)_{11}$. Subsequent excursion to 110 K again accelerates the conversion of terminal $Ru_3(CO)_{11}$(2-MeTHF) to CO-bridged $Ru_3(CO)_{11}$. Thus, accumulation of larger quantities of CO-bridged $Ru_3(CO)_{11}$ can be achieved by successive application of this procedure.

The $Ru_3(CO)_{11}$(2-MeTHF) and CO-bridged $Ru_3(CO)_{11}$ products do not accumulate during continuous near-UV irradiation of $Ru_3(CO)_{12}$ in a 90 K 2-MeTHF glass. After 5% photochemical conversion of $Ru_3(CO)_{12}$ at 90 K, there is IR spectral evidence for the accumulation of secondary photoproducts associated with loss of additional CO from terminal $Ru_3(CO)_{11}$(2-MeTHF). Eventually, up to three molecules of CO can be photoejected into the glass (2132 cm^{-1}) for every molecule of $Ru_3(CO)_{12}$ initially consumed. The accumulation of CO-bridged $Ru_3(CO)_{11}$ is never observed under these conditions, suggesting that the conversion of terminal $Ru_3(CO)_{11}$(2-MeTHF) to CO-bridged $Ru_3(CO)_{11}$ is not competitive with photochemical loss of CO from terminal $Ru_3(CO)_{11}$(2-MeTHF) in a 2-MeTHF glass. IR spectral features for secondary and tertiary photoproducts are not well understood, but subsequent reaction chemistry for these species suggest retention of the trinuclear metal framework. Warmup to 298 K of an extensively irradiated 90 K 2-MeTHF glass containing up to three photoejected CO's per $Ru_3(CO)_{12}$ molecule initially present results in quantitative regeneration of $Ru_3(CO)_{12}$. Warmup in the presence of 10 mM PPh_3 gives a mixture of $Ru_3(CO)_{12-n}(PPh_3)_n$ (n = 1, 2, 3) complexes in competition with significant regeneration of $Ru_3(CO)_{12}$. Mononuclear $Ru(CO)_4(PPh_3)$ and $Ru(CO)_3(PPh_3)_2$ products are not observed after warmup. These results support formulation of the photoproducts as $Ru_3(CO)_{12-n}$(2-MeTHF)$_n$ complexes with intact Ru_3 cores.

Extensive irradiation of a 2-MeTHF glass containing $Ru_3(CO)_{12}$ and CO-bridged $Ru_3(CO)_{11}$ yields conversion of the $Ru_3(CO)_{12}$

(41) Delley, B.; Manning, M. C.; Ellis, D. E.; Berkowitz, J.; Trogler, W. C. *Inorg. Chem.* **1982**, *21*, 2247–2253.
(42) Schilling, B. E. R.; Hoffman, R. *J. Am. Chem. Soc.* **1979**, *101*, 3456–3467.

to secondary and tertiary CO loss products without changing the concentration of CO-bridged $Ru_3(CO)_{11}$. Consistent with its formulation as a coordinatively unsaturated product in 2-MeTHF, CO-bridged $Ru_3(CO)_{11}$ is resistant to further photoinduced ligand loss while $Ru_3(CO)_{12}$ and the terminal form of $Ru_3(CO)_{11}$(2-MeTHF) rapidly lose CO. These results suggest initial photogeneration of equatorially substituted $Ru_3(CO)_{11}$(2-MeTHF) in the 90 K 2-MeTHF glass. While electronic factors favor isomerization of equatorially substituted $Ru_3(CO)_{11}$(2-MeTHF) to the axially substituted form, $Ru_3(CO)_{11}$(2-MeTHF) instead converts to CO-bridged $Ru_3(CO)_{11}$. In 2-MeTHF at 90 K, $Ru_3(CO)_{11}$ may adopt a delocalized vacancy which cannot bind 2-MeTHF. We find that the well-characterized $H_2Os_3(CO)_{10}$ complex[7,43,44] does not bind 2-MeTHF at 90 or 298 K and retains the low-energy electronic feature (λ (ϵ), nm (M^{-1} cm^{-1}): 535 (360) at 298 K; 524 (580) at 90 K in 2-MeTHF) associated with unsaturation delocalized by a four-center, $4e^-$ H_2Os_2 system. $Ru_3(CO)_{11}$ shows a significant selectivity for reaction with CO vs. the bulky PPh_3 ligand in alkane media. This behavior is proposed to be the consequence of delocalized unsaturation in $Ru_3(CO)_{11}$. Interestingly, regeneration of $Ru_3(CO)_{12}$ is more extensive in 2-MeTHF (80%) than in MCH (30%) for warmup of $Ru_3(CO)_{11}$ and photogenerated CO to 298 K in the presence of 10 mM PPh_3.

$Fe_3(CO)_{12}$. Near-UV irradiation of $Fe_3(CO)_{12}$ in a 90 K 2-MeTHF glass yields clean FTIR and UV–vis spectral changes which, unlike Ru, occur in constant ratio for significant extents (50%) of conversion and are consistent with photogeneration of the corresponding $Fe_3(CO)_{11}$(2-MeTHF) complex, Table I. This product, exhibiting two prominent absorptions at 1835 and 1783 cm^{-1}, is spectroscopically unrelated to CO-bridged $Ru_3(CO)_{11}$ in 2-MeTHF or $Fe_3(CO)_{11}$ in MCH and is perhaps related to the C_{2v} isomer of $Fe_3(CO)_{12}$ by substitution of 2-MeTHF for a terminal CO. The $Fe_3(CO)_{11}$(2-MeTHF) complex is spectroscopically distinct from the $Fe_3(CO)_{11}$(η^2-alkene) complexes, suggesting substitution at a different coordination site. Prolonged irradiation of $Fe_3(CO)_{11}$(2-MeTHF) in 2-MeTHF at 90 K yields photoejection of additional CO (2132 cm^{-1}) and the accompanying formation of FTIR detected (but unidentified) secondary photoproducts.

B. Long Wavelength Photochemistry of $Ru_3(CO)_{12}$ and $Fe_3(CO)_{12}$. (i) Associative Photosubstitution of $Ru_3(CO)_{12}$ and $Fe_3(CO)_{12}$ at 90 K. Having established the thermal reactivity of photogenerated $Ru_3(CO)_{11}$ (M = Ru, Fe) with CO, N_2, and C_2H_4 under kinetically controlled conditions in MCH glasses according to eq 3, we now consider the relative importance of dissociative CO loss vs. associative bimolecular photoreactions of $Ru_3(CO)_{12}$ in 90 K MP glasses, where these same entering groups can diffuse with similar relative mobilities (they all have the same molecular weight). Two important points are worth noting in these 90 K glasses: (i) photofragmentation products are never observed after prolonged irradiation and (ii) long wavelength (λ = 366- or 436-nm) photoexcitation of $Ru_3(CO)_{12}$ yields ^{13}CO exchange and C_2H_4 substitution *but not N_2 substitution.*

At 90 K, the first electronic absorption for $Ru_3(CO)_{12}$ (centered at 369 nm) is fairly well resolved from higher energy features. Excitation (366- or 436-nm) into this absorption yields negligible photochemistry in (a) an MCH glass, (b) an N_2-containing MP glass, and (c) a 2-MeTHF glass but rapidly yields $Ru_3(CO)_{11}$(η^2-alkene) complexes in (d) a C_2H_4-saturated MP glass or (e) a 1-pentene glass and yields $Ru_3(CO)_{12-n}(^{13}CO)_n$ complexes in (f) a ^{13}CO-saturated MP glass, as determined by FTIR. Irradiation (313-nm) of $Ru_3(CO)_{12}$ yields $Ru_3(CO)_{11}$ in glass (a) and $Ru_3(CO)_{11}L$ (L = N_2, 2-MeTHF, C_2H_4, C_5H_{10}, and ^{13}CO, respectively) complexes in glasses (b)–(f). Glasses (a)–(e) were irradiated identically with appropriately filtered light, and percent conversions, measured by FTIR spectroscopy, vary linearly with irradiation time at small extents (<10%) of photochemical conversion. Percent conversions [$C_i(\lambda)$], normalized to 5 min of irradiation, are reported in Table II.

Table II. Wavelength Dependent Disappearance Rates for Photoexcited $Ru_3(CO)_{12}$ and $Fe_3(CO)_{12}$

a. Normalized Disappearance Rates (% Decline) for 5 min of Filtered or Broad Band (Quartz) Irradiation of $Ru_3(CO)_{12}$ and $Fe_3(CO)_{12}$ at 90 K[a]

	normalized % decline[b]				
filter	(a) MCH	(b) MP/N_2	(c) 2-MeTHF	(d) MP/C_2H_4	(e) 1-pentene
			$Ru_3(CO)_{12}$		
436 nm	<0.01	<0.01	<0.01	3 (1)	9 (2)
366 nm	0.02 (1)	0.02 (1)	0.03 (1)	6 (1)	19 (3)
quartz	8 (2)	8 (2)	14 (3)	15 (3)	25 (5)
			$Fe_3(CO)_{12}$		
436 nm	0.10 (5)		0.10 (5)		5 (1)
Pyrex[c]	8 (2)		8 (2)		13 (2)

b. Previously Reported Quantum Yields for Photofragmentation (Φ_f) and Photosubstitution (Φ_s) of $Ru_3(CO)_{12}$ and $Fe_3(CO)_{12}$ in Octane Solution at 298 K

λ (nm)	conditions	$\Phi_f \times 10^3$	$\Phi_s \times 10^3$	ref
		$Ru_3(CO)_{12}$		
405	1 atm Ar	<0.1		21
405	0.012 M CO	28 ± 4		21
405	0.05 M C_2H_4	51 ± 5		21
405	0.012 M $P(OMe)_3$	23 ± 1		23
366	0.12 M $P(OMe)_3$	25 ± 1	34 ± 1	23
334	0.12 M $P(OMe)_3$	21 ± 1	68 ± 8	23
313	0.12 M $P(OMe)_3$	24 ± 2	86 ± 3	23
		$Fe_3(CO)_{12}$		
633	0.001 M PPh_3	10		3

[a] MCH = methylcyclohexane; MP = 3-methylpentane. The only product observed is $M_3(CO)_{11}L$ (L = MCH, N_2, 2-MeTHF, C_2H_4, C_5H_{10}). [b] Numbers in parentheses represent uncertainty in the least significant digit. [c] Pyrex transmits light of $\lambda > 280$ nm.

The photoreaction efficiencies are the same in glasses (a) and (b) suggesting that $Ru_3(CO)_{11}(N_2)$ formation in glass (b) is completely accounted for by the intermediacy of photogenerated $Ru_3(CO)_{11}$. Importantly, the C_2H_4 concentration (50 mM) in glass (d) is estimated to be about 10 times greater than the N_2 concentration (5 mM) in glass (b).[25] However, a concentration dependence alone is insufficient to account for the wavelength-dependent ratio of photosubstitution efficiencies (C_d/C_b (436 nm) > 300; C_d/C_b (366 nm) > 300; C_d/C_b (broad band) < 2) in these two glasses. These results suggest that low-energy excitation of $Ru_3(CO)_{12}$ generates a reactive isomer or excited state of $Ru_3(CO)_{12}$ which is trapped by C_2H_4 (and not by N_2) via an associative substitution pathway, while broad band excitation increases the efficiency for accumulation of $Ru_3(CO)_{11}$ as an intermediate in dissociative photosubstitution. The long wavelength photosubstitution pathway is important in a neat 1-pentene glass (e) (C_e/C_a (436 nm) > 1000, C_e/C_a (366 nm) > 1000) but not in a neat 2-MeTHF glass (c) (C_e/C_a (366 nm) = 1.5), Table II. Loss of CO becomes more competitive for broad band irradiation (C_e/C_c (broad band) < 2). With broad band irradiation, photosubstitution in a 2-MeTHF glass (c) is nearly twice as efficient as $Ru_3(CO)_{11}$ or $Ru_3(CO)_{11}(N_2)$ accumulation in the alkane glasses ((a) and (b), respectively), perhaps reflecting a change in the net cage escape efficiency for photoejected CO in the 2-MeTHF medium. The long wavelength photosubstitution of alkene for CO is 3 times more efficient in 1-pentene (e) than in C_2H_4-saturated MP (d) at 90 K, likely a consequence of larger alkene concentration in (e).

Long wavelength ($\lambda > 540$ nm) excitation into the first electronic absorption of $Fe_3(CO)_{12}$ (centered at 605 nm) yields no net photochemistry in alkane, 1-pentene, or 2-MeTHF glasses at 90 K. With 436-nm excitation, photoconversion in a neat 1-pentene glass (to form $Fe_3(CO)_{11}(\eta^2\text{-}C_5H_{10})$) is rapid on the time scale necessary to observe inefficient photoconversion in MCH (to form $Fe_3(CO)_{11}$) or 2-MeTHF (to form $Fe_3(CO)_{11}$(2-

(43) (a) Shapley, J. R.; Keister, J. B.; Churchill, M. R.; DeBoer, B. G. *J. Am. Chem. Soc.* **1975**, *97*, 4145–4145. (b) Broach, R. W.; Williams, J. M. *Inorg. Chem.* **1979**, *18*, 314–319.
(44) Deeming, A. J.; Hasso, S. *J. Organomet. Chem.* **1976**, *114*, 313–324.

MeTHF)) glasses, Table II. Pyrex-filtered irradiation yields similar photoconversion efficiencies for $Fe_3(CO)_{12}$ in all three glasses.

The wavelength- and medium-dependent photoconversion efficiencies for $Fe_3(CO)_{12}$ and $Ru_3(CO)_{12}$ at 90 K are clearly related. Selective irradiation into the second (first) electronic absorption for $Fe_3(CO)_{12}$ ($Ru_3(CO)_{12}$) enables associative photosubstitution by 1-pentene and not 2-MeTHF, whereas higher energy excitation is required to generate $M_3(CO)_{11}$ (M = Fe, Ru) in MCH. Clearly, the associative substitution pathway is favored for strong π-acceptor ligands as entering groups.

(ii) The Quenching of Photofragmentation of $Ru_3(CO)_{12}$ and $Fe_3(CO)_{12}$ at 90 K. The $Ru_3(CO)_{12}$ and $Fe_3(CO)_{12}$ complexes are known to undergo long wavelength photofragmentation in fluid solutions. However, attempts to observe photofragmentation of these clusters in rigid alkane glasses at 90 K have been without success. Near-UV irradiation of a 90 K MP glass containing ~0.1 mM $Ru_3(CO)_{12}$ or ~0.02 mM $Fe_3(CO)_{12}$ and ~10 mM free CO results in spectral changes identical with those observed in the absence of CO, yet limited conversion to the bridged form of $M_3(CO)_{11}$ results due to creation of a photostationary state which is a function of CO concentration (measured at 2132 cm^{-1}) and light intensity. Prolonged broad band irradiation with a 450-W medium pressure Hg lamp for 6 h maintains these photostationary states and leads to no additional spectral changes. In the dark, $Ru_3(CO)_{12}$ and $Fe_3(CO)_{12}$ are rapidly and quantitatively regenerated. Brief (<15 min) near-UV irradiation of $M_3(CO)_{12}$ (M = Ru, Fe) in ^{13}CO-containing MP glasses at 90 K yields rapid IR spectral changes consistent with accumulation of as many as eight photoejected ^{12}CO's per $M_3(CO)_{12}$ molecule initially present. In the dark, the UV–vis spectra return to coincidence with those obtained for the glass prior to irradiation. The final absorbance changes at 2132 cm^{-1} (generation of ^{12}CO) and at 2085 cm^{-1} (consumption of ^{13}CO) are of equal magnitude, suggesting that the extinction coefficients for ^{12}CO and ^{13}CO differ by less than 5% in MP at 90 K.

Near-UV irradiation of 0.1 mM $Ru_3(CO)_{12}$ or 0.02 mM $Fe_3(CO)_{12}$ in C_2H_4-saturated MP glasses at 90 K yields IR spectral changes consistent with rapid formation of $Ru_3(CO)_{11}(C_2H_4)$ or $Fe_3(CO)_{11}(C_2H_4)$, respectively. Prolonged irradiation yields secondary photoproducts associated with the photoejection of additional CO (2132 cm^{-1}). Similar behavior is observed for irradiation of $M_3(CO)_{12}$ (M = Ru, Fe) in neat 1-pentene glasses at 90 K. Mononuclear $M(CO)_{5-n}(\eta^2\text{-alkene})_n$ (M = Ru, Fe; n = 1–4) complexes[29] are never detected, again suggesting that photofragmentation is completely suppressed at 90 K. Secondary photoproducts are not observed during similar prolonged irradiation necessary to completely convert $Ru_3(CO)_{12}$ to $Ru_3(CO)_{11}(N_2)$ in an N_2-containing MP glass.

(iii) Solution Photochemistry of $Ru_3(CO)_{12}$ in Alkane Media at 195 K. Long wavelength (λ = 436-nm) photoexcitaton of $Ru_3(CO)_{12}$ in CO- or C_2H_4-saturated isooctane solutions at 298 K yields 3 equiv of $Ru(CO)_5$ or $Ru(CO)_4(C_2H_4)$, respectively, in accord with previous reports.[16] When these irradiated solutions are purged with Ar, $Ru_3(CO)_{12}$ is quantitatively regenerated in accord with the known lability of $Ru(CO)_5$[45] and $Ru(CO)_4(C_2H_4)$.[16,29] Photofragmentation quantum yields have previously been reported, Table II,[21] for 405-nm excitation of $Ru_3(CO)_{12}$ in octane solutions under 1 atm CO ([CO] = 0.012 M; Φ_f = 0.028 ± 4) or C_2H_4 ([C_2H_4] = 0.05 M; Φ_f = 0.051 ± 5). For solutions prepared under an Ar atmosphere, long wavelength photoexcitation yields $Ru(CO)_5$ at 298 K, but fragmentation yields are several orders of magnitude smaller, Table II. Long wavelength (λ > 420-nm) irradiation of $Ru_3(CO)_{12}$ in CO- or C_2H_4-saturated alkane solutions at 195 K enables detection of dinuclear intermediates associated with the fragmentation reactions of $Ru_3(CO)_{12}$. Importantly, $Ru_3(CO)_{12}$ exhibits negligible photochemistry in Ar-purged isooctane solutions at 195 K.

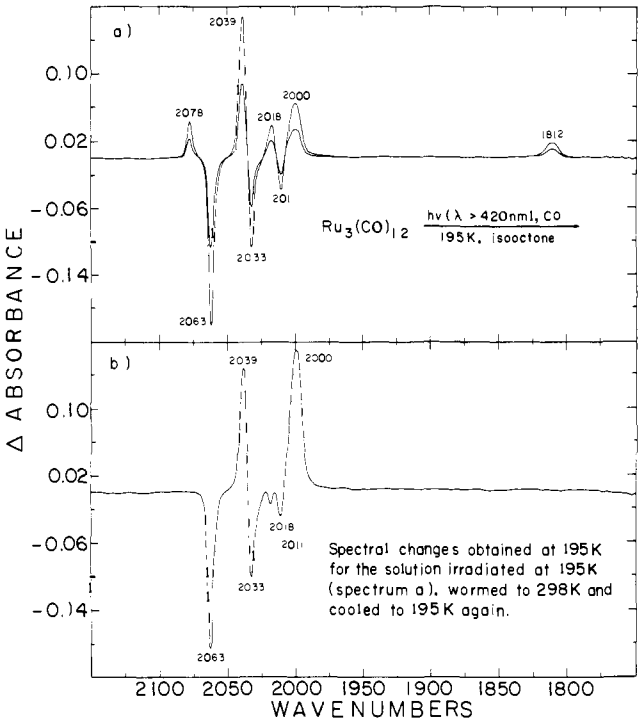

Figure 4. (a) IR difference spectral changes obtained after 20 and 40 min of long wavelength (λ > 420-nm) irradiation of 0.2 mM $Ru_3(CO)_{12}$ in a CO-saturated isooctane solution at 195 K. The negative absorbance changes are associated with consumption of $Ru_3(CO)_{12}$, while positive absorbances changes are attributed to $Ru(CO)_5$ [ν (cm^{-1}) = 2037, 2000 in isooctane at 195 K] and $Ru_2(CO)_9$ [ν (cm^{-1}) = 2078, 2039, 2029, 2018, 2006, 1812 in isooctane at 195 K]. (b) The IR difference spectrum was obtained at 195 K for the solution irradiated at 195 K (spectrum a), warmed to 298 K, and recooled to 195 K. Negative deviations are associated with irreversibly consumed $Ru_3(CO)_{12}$, while positive deviations are attributed to $Ru(CO)_5$.

Long wavelength (λ > 420-nm) photoexcitation of ~0.2 mM $Ru_3(CO)_{12}$ in a CO-saturated isooctane solution at 195 K yields clean FTIR spectral changes shown in Figure 4a. The IR spectral changes in Figure 4a show decline of absorption for $Ru_3(CO)_{12}$ (ν (ϵ), cm^{-1} (M^{-1} cm^{-1}); 2063 (33 500), 2031 (24 500), 2017 (5000), 2011 (11 000) in isooctane at 195 K), growth of a prominent absorption at 1812 cm^{-1}, and growth of a number of bands in the region where $Ru_3(CO)_{12}$ absorbs. Photochemical consumption of $Ru_3(CO)_{12}$ can be determined quantitatively by monitoring at 2063 cm^{-1}, where product features do not absorb. The time evolution of these photoproduct absorptions is consistent with initial photoproduction of equal amounts of $Ru(CO)_5$ (ν (ϵ), cm^{-1} (M^{-1} cm^{-1}); 2037 (9300), 2000 (10 400) in isooctane at 195 K) and $Ru_2(CO)_9$ (ν (ϵ), cm^{-1} (M^{-1} cm^{-1}); 2078 (7500), 2039 (20 500), 2029 (5100), 2018 (10 000), 2006 (2100), 1812 (3300) in isooctane at 195 K) according to eq 4. Inefficient photo-

$$Ru_3(CO)_{12} \xrightarrow[195\ K,\ isooctane]{h\nu\ (\lambda > 420\ nm),\ CO} Ru(CO)_5 + Ru_2(CO)_9 \quad (4)$$

fragmentation of photogenerated $Ru_2(CO)_9$ leads to a small increase in the $Ru(CO)_5$ product yield from 1.0 to 1.1 during 40 min of λ > 420-nm irradiation at 195 K, Figure 4a. The $Ru(CO)_5$ complex does not absorb appreciably at λ > 420 nm, and higher energy excitation is required to inefficiently yield $Ru_2(CO)_9$ and some $Ru_3(CO)_{12}$ from 195 K irradiation of independently prepared $Ru(CO)_5$-containing solutions. These results for $Ru(CO)_5$ accord well with a previous report which attributes spectral features at 2078, 2039, and 1812 cm^{-1} to photogenerated $Ru_2(CO)_9$.[46] Thus, $Ru_2(CO)_9$ appears to be a direct product of long wavelength photoexcitation of $Ru_3(CO)_{12}$ in CO-saturated alkane solution at 195 K. Warmup to 298 K of the irradiated 195 K solution

(45) (a) Manchot, W.; Manchot, W. J. *Z. Anorg. Allg. Chem.* **1936**, *226*, 385–415. (b) Calderazzo, F.; L'Eplattenier, F. *Inorg. Chem.* **1967**, *6*, 1220–1224.

(46) Moss, J. R.; Graham, W. A. G. *J. Chem. Soc., Dalton Trans.* **1977**, 95–99.

yields IR spectral changes which persist on recooling the solution to 195 K, Figure 4b, consistent with ~6% regeneration of $Ru_3(CO)_{12}$ (2063 cm^{-1}) and conversion of $Ru_2(CO)_9$ (1812 cm^{-1}) to $Ru(CO)_5$ (2000 cm^{-1}). Subsequent purging with Ar at 298 K quantitatively regenerates $Ru_3(CO)_{12}$, establishing a quantitative spectroscopic yield of $Ru(CO)_5$ in Figure 4b and in turn establishing the initial photogeneration of one molecule of $Ru(CO)_5$ (determined at 2000 cm^{-1}) for every molecule of $Ru_3(CO)_{12}$ consumed (determined at 2063 cm^{-1}) in the original 195 K irradiation (Figure 4a). Deconvolution of IR spectral features for $Ru_3(CO)_{12}$ and $Ru(CO)_5$ in Figure 4a enables clean resolution of the remaining product features associated with photogenerated $Ru_2(CO)_9$. The IR spectral features for $Ru_2(CO)_9$ establish, for the first time, that $Ru_2(CO)_9$ is isostructural with $Os_2(CO)_9$,[46] clearly ruling out an $Fe_2(CO)_9$-type structure.

In a C_2H_4-saturated solution at 195 K, long wavelength ($\lambda >$ 420 nm) photoexcitation of ~0.2 mM $Ru_3(CO)_{12}$ yields FTIR spectral changes, presented as Supplementary Material. The growth of a bridging CO feature at 1805 cm^{-1} is accompanied by the growth of terminal CO features in the region of declining spectral features for $Ru_3(CO)_{12}$. The ratio of intensities of the product spectral features changes during the irradiation, thus enabling distinction of IR spectral features for $Ru(CO)_4(C_2H_4)$ (ν (ϵ); cm^{-1} (M^{-1} cm^{-1}): 2106 (1200), 2024 (14 000), and 1996 (7500) in isooctane at 195 K) and a CO-bridged product (ν (rel abs); cm^{-1}: 2114 (0.03), 2109 (0.03), 2065 (2.2), 2030 (5.2), 2017 (3.7), 2004 (2.0), 1805 (1.0)). During 12 min of irradiation, the spectroscopic yield of $Ru(CO)_4(C_2H_4)$ increases from 1.0 to 1.2 at the expense of product features for the CO-bridged product.

Warmup to 298 K of the irradiated 195 K solution yields IR spectral changes which persist on recooling and which remain unchanged in the dark at 195 K, consistent with 44% regeneration of $Ru_3(CO)_{12}$ and conversion of remaining CO-bridged product to $Ru(CO)_4(C_2H_4)$. Warmup to 298 K eventually regenerates $Ru_3(CO)_{12}$ quantitatively, establishing a quantitative spectroscopic yield for $Ru(CO)_4(C_2H_4)$. These stoichiometric considerations suggest (i) formulation of the CO-bridged product as $Ru_2(CO)_8(C_2H_4)$, Table I, and (ii) long wavelength 195 K photofragmentation of $Ru_3(CO)_{12}$ according to eq 5. The $Ru_2(CO)_8(C_2H_4)$ fragments in C_2H_4-saturated alkane solutions at 195 K according to eq 6. Pyrex-filtered ($\lambda >$ 280-nm) irradiation

$$Ru_3(CO)_{12} \xrightarrow[195\ K,\ isooctane]{h\nu\ (\lambda > 420\ nm),\ C_2H_4} Ru_2(CO)_8(C_2H_4) + Ru(CO)_4(C_2H_4) \quad (5)$$

$$Ru_2(CO)_8(C_2H_4) \xrightarrow[195\ K,\ alkane]{h\nu,\ C_2H_4} 2Ru(CO)_4(C_2H_4) \quad (6)$$

of another aliquot of the same solution yields IR spectral changes consistent with the additional accumulation of $Ru_3(CO)_{11}(C_2H_4)$, Table I, as an additional photoproduct at 195 K. $Ru_3(CO)_{11}(C_2H_4)$ slowly reacts with liberated CO to regenerate $Ru_3(CO)_{12}$ in the dark at 195 K.

Long wavelength ($\lambda >$ 420-nm) photoexcitation of $Ru(CO)_4(C_2H_4)$ (there is negligible absorption at such wavelengths) in an independently prepared C_2H_4-saturated solution at 195 K yields no net chemistry while higher energy excitation yields stable solutions of $Ru(CO)_3(C_2H_4)_2$ and eventually *trans*-$Ru(CO)_2(C_2H_4)_3$.[29] The 1805-cm^{-1} feature for $Ru_2(CO)_8(C_2H_4)$ is never observed during such irradiations. The IR spectral features for $Ru_2(CO)_8(C_2H_4)$ are different from those for $Os_2(CO)_8(\mu\text{-}\eta^1,\eta^1\text{-}H_2CCH_2)$.[47] $Ru_2(CO)_8(C_2H_4)$ may be structurally related to $Ru_2(CO)_9$ by replacement of one terminal CO ligand by C_2H_4. Attempts to characterize $Ru_2(CO)_8(C_2H_4)$ by ^1H NMR spectroscopy at 195 K have been unsuccessful.

Long wavelength (λ = 436-nm) photoexcitation of ~0.2 mM $Ru_3(CO)_{12}$ in a PPh_3-containing isooctane solution at 298 K initially yields (<5% conversion) 2.6 $Ru(CO)_4(PPh_3)$ and 0.4 $Ru(CO)_3(PPh_3)_2$ as the only FTIR detected photoproducts, independent of PPh_3 concentration (1–100 mM). $Ru_3(CO)_{11}(PPh_3)$ is observed as an additional product of 313- or 366-nm excitation. Photofragmentation quantum yields are reportedly insensitive to irradiation wavelength, while competitive photosubstitution quantum yields increase with increasing excitation energy, Table II.[23]

Long wavelength ($\lambda >$ 420-nm) irradiation of 0.2 mM $Ru_3(CO)_{12}$ in a PPh_3-containing isooctane solution at 195 K yields initial formation of a CO-bridged (1791 cm^{-1}) intermediate X, Table I. In the dark at 195 K, spectral features for both $Ru_3(CO)_{11}(PPh_3)$ and $Ru_3(CO)_{12}$ grow at the expense of those for intermediate X, in a ratio which increases with increasing PPh_3 concentration. These results suggest retention of the Ru_3 core in intermediate X. As the 195 K irradiation proceeds, the relative yield of this initially observed intermediate declines in apparent correlation with an increase, from initial values near zero, in the relative yields of $Ru(CO)_4(PPh_3)$, $Ru(CO)_3(PPh_3)_2$, and predominantly $Ru_3(CO)_{11}(PPh_3)$. Continued irradiation eventually yields decline of $Ru_3(CO)_{11}(PPh_3)$, an increase in the $Ru(CO)_3(PPh_3)_2/Ru(CO)_4(PPh_3)$ product ratio from an initial value of ~0.15, and corresponding generation of a second CO-bridged (1768 cm^{-1}) intermediate. Warmup to 298 K of the irradiated 195 K solutions leads to a complete decline of the two bridging carbonyl features, significant regeneration of $Ru_3(CO)_{12}$, retention (low [PPh_3]) or partial decline (high [PPh_3]) in the spectroscopic yield of $Ru_3(CO)_{11}(PPh_3)$, and generation of more $Ru(CO)_4(PPh_3)$ and $Ru(CO)_3(PPh_3)_2$. The $Ru(CO)_3(PPh_3)_2/Ru(CO)_4(PPh_3)$ product ratio always increases during the warmup but never exceeds a ratio of 0.5. Greater accumulation of the second CO-bridged photoproduct (1768 cm^{-1}) at 195 K leads to higher yields of $Ru(CO)_3(PPh_3)_2$ on warmup to 298 K. Low concentrations of PPh_3 and low extents of conversion at 195 K both contribute to more efficient regeneration of $Ru_3(CO)_{12}$ during warmup, due to back reaction of intermediate X (1791 cm^{-1}). In summary, long wavelength photoexcitation of $Ru_3(CO)_{12}$ in a PPh_3-containing alkane solution at 195 K appears to yield an unidentified Ru_3 species. Fragmentation products in the presence of PPh_3 result only from secondary reactions.

(iv) **Solution Photochemistry of $Fe_3(CO)_{12}$.** Previous reports have established that low-energy visible light excitation of $Fe_3(CO)_{12}$[27] yields extraordinarily fast 1-pentene isomerization. These reports have prompted a more detailed investigation of the products of fragmentation of $Fe_3(CO)_{12}$ in alkane solutions containing excess C_2H_4. Long wavelength photoexcitation ($\lambda >$ 540 nm) of $Fe_3(CO)_{12}$ in a CO-saturated MP solution at 298 K yields IR spectral changes consistent with quantitative photoconversion to 3 equiv of $Fe(CO)_5$. Similar irradiation of 0.2 mM $Fe_3(CO)_{12}$ in a PPh_3-containing MP solution at 298 K yields spectral changes consistent with photoconversion to a mixture of $Fe(CO)_5$, $Fe(CO)_4(PPh_3)$, $Fe(CO)_3(PPh_3)_2$, and minor amounts of $Fe_3(CO)_{11}(PPh_3)$. Photogenerated $Fe_3(CO)_{11}(PPh_3)$ fragments in the dark at 298 K to yield additional $Fe(CO)_4(PPh_3)$ and $Fe(CO)_3(PPh_3)_2$ but not $Fe(CO)_5$. At high concentrations of PPh_3 (0.1 M), $Fe_3(CO)_{11}(PPh_3)$ is not detected, and photofragmentation product distributions are as indicated in eq 7. Photofragmentation

$$Fe_3(CO)_{12} \xrightarrow[298\ K,\ MP]{h\nu\ (\lambda > 540\ nm),\ PPh_3} 0.7Fe(CO)_5 + 1.2Fe(CO)_4(PPh_3) + 1.1Fe(CO)_3(PPh_3)_2 \quad (7)$$

quantum yields have been reported,[3] Table II, for 633-nm irradiation of $Fe_3(CO)_{12}$ in isooctane solutions containing 1 mM PPh_3 (Φ_f = 0.01). While $\lambda >$ 540-nm irradiation of $Fe_3(CO)_{12}$ in PPh_3-containing solutions at 195 K yields the same mononuclear products observed at 298 K, $Fe_3(CO)_{11}(PPh_3)$ is also accumulated in >20% yield. Furthermore, mononuclear product features decline, and the ratio of absorbance changes at 2086 cm^{-1} (production of $Fe_3(CO)_{11}(PPh_3)$) and 2047 cm^{-1} ($Fe_3(CO)_{12}$ consumption) increases with decreasing irradiation wavelength for 436-, 366-, and 313-nm irradiation. In summary, the $Fe(CO)_5$, $Fe(CO)_4(PPh_3)$, and $Fe(CO)_3(PPh_3)_2$ complexes form by direct photofragmentation of $Fe_3(CO)_{12}$, while $Fe(CO)_4(PPh_3)$ and $Fe(CO)_3(PPh_3)_2$ are additionally formed by fragmentation of photogenerated $Fe_3(CO)_{11}(PPh_3)$. Importantly, $Fe(CO)_5$ is not

(47) Motyl, K. M.; Norton, J. R.; Schauer, C. K.; Anderson, O. P. *J. Am. Chem. Soc.* **1982**, *104*, 7325–7327.

formed when photogenerated $Fe_3(CO)_{11}$ is warmed to 298 K in the presence of PPh_3.

Long wavelength ($\lambda > 540$ nm) excitation of $Fe_3(CO)_{12}$ in a C_2H_4-saturated MP solution at 298 K yields clean IR spectral changes presented as Supplementary Material. All absorbance changes occur in constant ratio throughout the photoconversion and are subsequently persistent in the dark for several hours. The IR spectral changes show decline of absorption features for $Fe_3(CO)_{12}$ and growth of prominent new features at 2088, 2023, 2008, 2001, and 1984 cm^{-1}. Similar IR spectral changes accompany $\lambda > 540$-nm excitation of $Fe_3(CO)_{12}$ in a C_2H_4-saturated $CF_3C_6F_{11}$ solution at 298 K. Corresponding ^1H NMR spectral changes (C_7H_{14} used at internal standard: 1.54 ppm vs. $SiMe_4$) in $CF_3C_6F_{11}$ indicate growth of two prominent singlets in a constant 1:2 ratio of integrated intensities at 2.37 ($Fe(CO)_4(C_2H_4)$) and 2.68 ($Fe(CO)_3(C_2H_4)_2$) ppm vs. $SiMe_4$. Corresponding UV–vis spectral changes indicate complete decline of intense low-energy electronic spectral features for $Fe_3(CO)_{12}$ at 602, 437 (sh), and 360 nm (sh). No new low-energy electronic features grow in for the accumulated photoproducts suggesting complete fragmentation of the Fe_3 core of $Fe_3(CO)_{12}$ to yield mononuclear products. The 2023- and 2001-cm^{-1} product features indicate formation of $Fe(CO)_5$ [IR (MP, 298 K) ν (ϵ), cm^{-1} (M^{-1} cm^{-1}) 2023 (10000), 2001 (14300)]. The product features at 2088 and 2008 cm^{-1} and 2.37 ppm are due to formation of $Fe(CO)_4(C_2H_4)$ [IR (MP, 298 K) ν (ϵ), cm^{-1} (M^{-1} cm^{-1}) 2088 (1700), 2014 sh, 2008 (12800), 1986 (8400); ^1H NMR (250 MHz, $CF_3C_6F_{11}$, 298 K) 2.37 (s)], while the product feature at 2.68 ppm indicates formation of $Fe(CO)_3(C_2H_4)_2$ [IR (MP, 298 K) ν (ϵ), cm^{-1} (M^{-1} cm^{-1}) 2060 (940), 1990 (5100), 1983 (12600); ^1H NMR (250 MHz, $CF_3C_6F_{11}$, 298 K) 2.68 (s)].[29]

The IR difference spectral changes for the photofragmentation of $Fe_3(CO)_{12}$ in C_2H_4-saturated MP were simulated, Figure 5, by optimization of the coefficients of digital summation of independently generated FTIR spectra for each component in the MP mixture. Extinction coefficients for $Fe_3(CO)_{12}$ and $Fe(CO)_5$ were determined by direct methods and shown to be self-consistent by comparison to IR spectral changes accompanying the long wavelength ($\lambda > 540$-nm) photoconversion of $Fe_3(CO)_{12}$ quantitatively to $Fe(CO)_5$ in a CO-saturated MP solution at 298 K. Clean solutions of $Fe(CO)_4(C_2H_4)$ were prepared by irradiating $Fe(CO)_5$ in a C_2H_4-saturated solution and then purging the solution with CO.[29] Irradiation of $Fe(CO)_4(C_2H_4)$ in a C_2H_4-purged MP solution initially yields $Fe(CO)_3(C_2H_4)_2$, a reaction which is reversed under CO.[29] Quantitation of IR spectral changes for the net conversion of $Fe(CO)_5$ to $Fe(CO)_4(C_2H_4)$ and for the reversible interconversion of $Fe(CO)_3(C_2H_4)_2$ and $Fe(CO)_4(C_2H_4)$ allows estimation of extinction coefficients for $Fe(CO)_3(C_2H_4)_2$ and $Fe(CO)_4(C_2H_4)$ based on the extinction coefficients for $Fe(CO)_5$. Relative molar absorptivities obtained by FTIR spectroscopy for $Fe_3(CO)_{12}$, $Fe(CO)_4(C_2H_4)$, $Fe(CO)_5$, and $Fe(CO)_3(C_2H_4)_2$ in independently prepared MP solutions at 298 K have been multiplied by optimized stoichiometric coefficients (−1.00, 0.97, 1.01, 0.98, respectively) to yield weighted relative molar absorptivities shown in Figure 5a, such that digital summation yields a simulated IR difference spectrum (Figure 5b) which is virtually indistinguishable from that obtained experimentally at low (3%) extent photochemical conversion of $Fe_3(CO)_{12}$ to the mononuclear products (Figure 5c). With a stoichiometric coefficient of −1.00 for $Fe_3(CO)_{12}$, the remaining coefficients were determined by serially optimizing the fit at 2088, 2023 or 2001, and 1984 cm^{-1} for $Fe(CO)_4(C_2H_4)$, $Fe(CO)_5$, and $Fe(CO)_3(C_2H_4)_2$, respectively. The optimized stoichiometric coefficients account for 99% of the $Fe_3(CO)_{12}$ consumed during irradiation and agree with the ^1H NMR data, which also indicate photogeneration of $Fe(CO)_4(C_2H_4)$ and $Fe(CO)_3(C_2H_4)_2$ in a 1:1 molar ratio. In summary, long wavelength photofragmentation of $Fe_3(CO)_{12}$ proceeds according to eq 8 in C_2H_4-saturated alkane

$$Fe_3(CO)_{12} \xrightarrow[298\ K,\ MP]{h\nu\ (\lambda > 540\ nm),\ C_2H_4} Fe(CO)_5 + Fe(CO)_4(C_2H_4) + Fe(CO)_3(C_2H_4)_2 \quad (8)$$

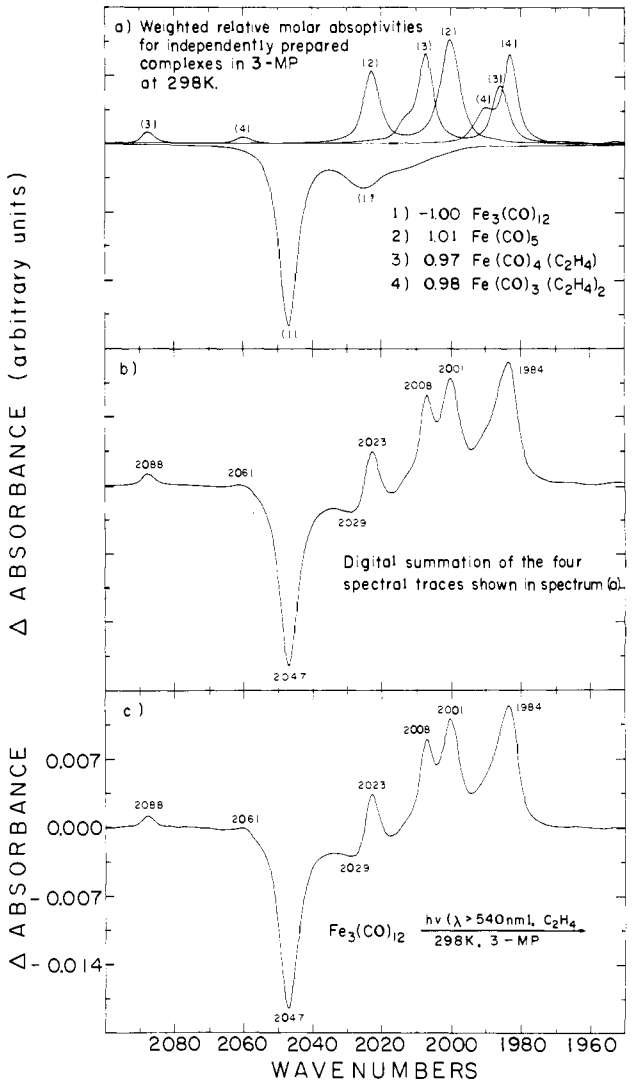

Figure 5. (a) Weighted relative molar absorptivities for (1) $Fe_3(CO)_{12}$, (2) $Fe(CO)_5$, (3) $Fe(CO)_4(C_2H_4)$, and (4) $Fe(CO)_3(C_2H_4)_2$ in independently prepared MP solutions at 298 K. The optimized stoichiometric coefficients shown were chosen such that the digital summation of these four spectral traces yields the simulated IR difference spectrum (b) which is in closest agreement with the experimentally obtained IR difference spectral changes (c) associated with long wavelength ($\lambda > 540$-nm) irradiation (3% conversion) of $Fe_3(CO)_{12}$ in a C_2H_4-saturated MP solution at 298 K.

solutions at 298 K. Competitive photosubstitution also yields $Fe_3(CO)_{11}(C_2H_4)$ at 195 K. Consistent with results for photoreaction of $Fe_3(CO)_{12}$ in the presence of C_2H_4, long wavelength ($\lambda > 540$ nm) photoexcitation of 0.2 mM $Fe_3(CO)_{12}$ in a C_3H_6-saturated MP solution yields IR spectral changes consistent with photogeneration of nearly equal quantities of $Fe(CO)_5$, $Fe(CO)_4(C_3H_6)$, and $Fe(CO)_3(C_3H_6)_2$.

Discussion

Structure and Reactivity of $M_3(CO)_{11}$ (M = Ru, Fe). Figure 6 summarizes our current understanding of the nature of photogenerated $Ru_3(CO)_{11}$, which initially adopts a structure with all terminal CO's, II, and slowly isomerizes at 90 K to a more stable, bridged form, III. The structure of III (M = Ru, Fe) cannot be determined with certainty from the available IR data but may be related to the structure presented in Figure 6. IR spectral comparison of $M_3(CO)_{11}$ complexes indicates that photogenerated $Os_3(CO)_{11}$[24] and $Fe_3(CO)_{11}$ adopt geometries closely related to those for II and III, respectively. The FTIR detected terminal form of $Os_3(CO)_{11}$ and the bridged form of $Ru_3(CO)_{11}$ both react with ^{13}CO at 110 K quantitatively to yield axial-^{13}CO–$M_3(CO)_{11}(^{13}CO)$ complexes. These results serve to support

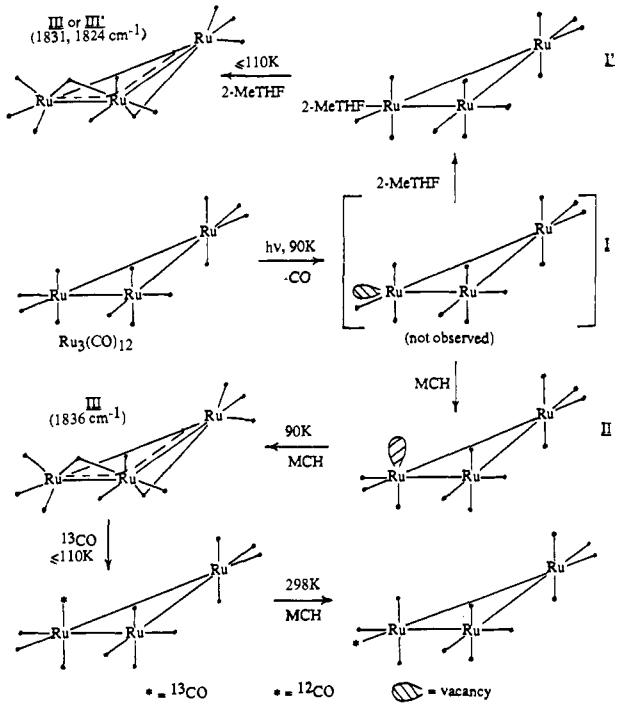

Figure 6. Summary of the structural and chemical nature of photogenerated $Ru_3(CO)_{11}$.

description of II (M = Os, Ru) as structurally related to $M_3(CO)_{12}$ by net creation of an axial (orthogonal to the trinuclear metal framework) vacancy. The IR spectral features support this description for axially vacant II (M = Ru, Os).[24] The results further suggest that an axial vacancy is retained upon isomerization of $Ru_3(CO)_{11}$ from II to III.

Detection of equatorially substituted $Ru_3(CO)_{11}$(2-MeTHF), I', as an intermediate leading to formation of $Ru_3(CO)_{11}$ in a 2-MeTHF glass suggests initial loss of equatorial CO from $Ru_3(CO)_{12}$ to form equatorially vacant $Ru_3(CO)_{11}$ (I). In the absence of a $2e^-$ donor ligand such as 2-MeTHF, I rapidly isomerizes to II and then more slowly to III. The photodissociation of equatorial CO has been established for $Os_3(CO)_{12}$[24] by showing selective photochemical loss of ^{12}CO from the axial-^{13}CO–$Os_3(CO)_{11}(^{13}CO)$. For Ru, photoisomerization of the $Ru_3(CO)_{11}(^{13}CO)$ isomers is rapid on the time scale necessary to observe CO loss at 90 K.

Recently, $\lambda > 315$-nm irradiation of $Ru_3(CO)_{12}$ in THF solution at 298 K was shown to yield a transient, formulated as $Ru_3(CO)_{11}$(THF), exhibiting UV–vis spectral features[23] very similar to those for $Ru_3(CO)_{11}$(2-MeTHF) (I') in 2-MeTHF at 90 K. The kinetic properties of $Ru_3(CO)_{11}$(THF) at 298 K[23] suggest a reversible equilibrium with $Ru_3(CO)_{11}$. We find for the more bulky 2-MeTHF ligand that this equilibrium favors $Ru_3(CO)_{11}$ (III) at 90 K. The kinetic data at 298 K further suggest that $Ru_3(CO)_{11}$ reacts preferentially with CO vs. the more bulky $P(OCH_3)_3$ or PPh_3 ligands at 298 K.[23] This behavior has been proposed[23] to be the consequence of delocalized unsaturation in $Ru_3(CO)_{11}$. Accordingly, we observe preferential uptake of CO vs. PPh_3 on warmup of 90 K alkane glasses containing photogenerated $Ru_3(CO)_{11}$, photoejected CO, and excess PPh_3. The preferential uptake of CO is even more pronounced in 2-MeTHF. For $M_3(CO)_{11}$ (III), we favor a bridging structure in which the unsaturation is delocalized. A delocalized vacancy would stabilize $Ru_3(CO)_{11}$ (III) in a 2-MeTHF glass as suggested by the IR spectral data.

Spectroscopic data for III indicate that more than one bridging CO is involved in delocalization of the unsaturation. Furthermore, the unsaturation is delocalized in such a fashion that III reacts with ^{13}CO to yield axial-^{13}CO–$Ru_3(CO)_{11}(^{13}CO)$. The structure proposed in Figure 6 for III is consistent with all of these considerations. Structure III in Figure 6 exhibits the undecacarbonyl ligand set geometry that would obtain upon elongation of the longest Fe–C bond for the triply bridging CO in the crystallographically characterized $[Fe_3(CO)_{11}]^{2-}$ dianion.[48] The terminal $M_3(CO)_9$ ligand sets for crystallographically characterized $Ru_3(CO)_9(\mu^3\text{-}CO)(\mu^3\text{-}NR)$ complexes [R = Ph,[49] $SiMe_3$[50]] are related to that for structure III and give IR spectral features similar to those observed for CO-bridged $Ru_3(CO)_{11}$. An attractive alternative structure for $Ru_3(CO)_{11}$, where the coordinative unsaturation is delocalized by having one equatorial CO bridge an edge of the metal triangle {cf. $RuCo_2(\mu\text{-}CO)(CO)_{10}$,[51] $OsCo_2(CO)_{11}$,[52] $[Ru_3(CO)_{11}]^{2-}$,[53] and $[Os_3(CO)_{11}]^{2-}$[54]}, is *not* consistent with our present characterization of bridged $Ru_3(CO)_{11}$ since it contains only one bridging CO and is not expected to react with ^{13}CO to yield axial-^{13}CO–$Ru_3(CO)_{11}(^{13}CO)$.

Attempts have recently been made to explain the structures of metal carbonyl clusters in terms of packing of the CO ligands to give the lowest energy polyhedron which can accommodate the metal skeleton.[55] The CO's of $Fe_3(CO)_{12}$ form a crystallographically characterized[35] icosahedral array but are forced to adopt the less favored anticuboctahedron in $Os_3(CO)_{12}$[56] in order to enclose the larger Os_3 triangle. IR spectral evidence for $Ru_3(CO)_{12}$ suggests that the Ru_3 core is capable of accommodating both ligand arrays,[57] and crystallographic data confirm anticuboctahedral and icosahedral ligand arrays in $Ru_3(CO)_{12}$[58] and $Ru_3(CO)_{11}(CNBu^t)$,[59] respectively. Removal of one CO from $M_3(CO)_{12}$ (M = Ru, Os) at 90 K yields an anticuboctahedron-1 ligand array, proposed for terminal forms of $Os_3(CO)_{11}$ (I and II). Alternatively, removal of one CO from $Fe_3(CO)_{12}$ yields an icosahedral-1 ligand array proposed in structure III and observed for the structurally characterized $[Fe_3(\mu^3\text{-}CO)(\mu^2\text{-}CO)(CO)_9]^{2-}$ dianion.[48] The isomerization of $Ru_3(CO)_{11}$ from II to III suggests a restructuring of the ligand array from anticuboctahedral-1 to a less spacious icosahedral-1 ligand array on the laboratory time scale. Alternatively, the rapid conversion from I to II is driven by electronic factors, without collapse of the spacious anticuboctahedral-1 ligand array.

Wavelength-Dependent Photochemistry of $M_3(CO)_{12}$: Fragmentation vs. CO Loss. Results presented here and elsewhere[23] indicate that the rate of internal conversion in $M_3(CO)_{12}$ complexes (M = Fe, Ru, Os) is only competitive with the rate of reaction from upper excited states. In accord with recent findings of Ford and co-workers,[23] the present study shows that longer wavelength ($\lambda > 420$ nm) excitation of $Ru_3(CO)_{12}$ in the presence of CO, C_2H_4, or PPh_3 leads almost exclusively to inefficient photofragmentation into mononuclear complexes at 298 K, while higher energy excitation leads to significant photosubstitution of the intact cluster by PPh_3. Similar behavior has been established[24] for $Os_3(CO)_{12}$. While net photofragmentation dominates the photochemistry of $Fe_3(CO)_{12}$ in fluid solution at 298 K,[3] even in the absence of added ligands,[17] we find that irradiation of $Fe_3(CO)_{12}$ in PPh_3-containing alkane solutions at 195 K yields both substitution ($Fe_3(CO)_{11}(PPh_3)$) and fragmentation ($Fe(CO)_{5-n}(PPh_3)_n$

(48) Lo, F. Y.-K.; Longoni, G.; Chini, P.; Lower, L. D.; Dahl, L. F. *J. Am. Chem. Soc.* **1980**, *102*, 7691–7701.
(49) Sappa, E.; Milone, L. *J. Organomet. Chem.* **1973**, *61*, 383–388.
(50) Abel, E. W.; Blackmore, T.; Whittey, R. J. *Inorg. Nucl. Chem. Lett.* **1974**, *10*, 941–944.
(51) Roland, E.; Vahrenkamp. H. *Angew. Chem., Int. Ed. Engl.* **1981**, *20*, 679–680.
(52) Moss, J. R.; Graham, W. A. G. *J. Organomet. Chem.* **1970**, *23*, C23–C24.
(53) Bhattacharyza, A. A.; Nagel, C. C.; Shore, S. G. *Organometallics* **1983**, *2*, 1187–1193.
(54) Nagel, C. C.; Bricker, J. C.; Alway, D. G.; Shore, S. G. *J. Organomet. Chem.* **1981**, *219*, C9–C12.
(55) Benfield, R. E.; Johnson, B. F. G. *Transition Met. Chem.* **1981**, *6*, 131. Benfield, R. E.; Johnson, B. F. G. *J. Chem. Soc., Dalton Trans.* **1980**, 1743–1767.
(56) Churchill, M. R.; DeBoer, B. G. *Inorg. Chem.* **1977**, *16*, 878–884.
(57) Bentsen, J. G.; Wrighton, M. S., unpublished results.
(58) (a) Mason, R.; Rae, A. I. M. *J. Chem. Soc. A* **1968**, 778–779. (b) Churchill, M. R.; Hollander, F. J.; Hutchinson, J. P. *Inorg. Chem.* **1977**, *16*, 2655–2659.
(59) Bruce, M. I.; Matisons, J. G.; Wallis, R. C.; Patrick, J. M.; Skelton, B. W.; White, A. H. *J. Chem. Soc., Dalton Trans.* **1983**, 2365–2373.

(n = 0–2)) products. Here again, photosubstitution is more important for higher energy excitation. Photosubstitution efficiencies in fluid solution support a wavelength dependent loss of CO from $M_3(CO)_{12}$ complexes. Photofragmentation is completely suppressed in organic glasses at 90 K, thus enabling accumulation of photogenerated $M_3(CO)_{11}$, according to eq 1, upon near-UV promotion of a higher energy electronic transition(s).

Excitation into the overlapping second and third electronic absorptions for $Ru_3(CO)_{12}$ or the third electronic absorption for $Os_3(CO)_{12}$[24] and $Fe_3(CO)_{12}$ gives (i) dissociative loss of CO in an alkane glass at 90 K, (ii) dissociative substitution of L for CO (L = ^{13}CO, C_2H_4, C_5H_{10}, N_2 (Ru, Os only), and 2-MeTHF) at 90 K, and (iii) wavelength-dependent substitution of PPh_3 for CO in fluid solution. In accord with the nature of the third allowed electronic transition ($\sigma^{*\prime} \rightarrow \sigma^*$, $d_{x^2-y^2} \rightarrow d_{xy}$)[41] the selective photochemical extrusion of a nonstatistical excess of ^{12}CO from axial-^{13}CO–$Os_3(CO)_{11}(^{13}CO)$ and the kinetic trapping of equatorially substituted $Ru_3(CO)_{11}$(2-MeTHF) suggest preferential loss of equatorial CO from $Os_3(CO)_{12}$ and $Ru_3(CO)_{12}$.

Spectroscopic investigations[19] indicate that the second allowed electronic transitions of $Fe_3(CO)_{12}$ and $Os_3(CO)_{12}$ and the first allowed electronic transition of $Ru_3(CO)_{12}$ approximate a $\sigma \rightarrow \sigma^*$ transition. Promotion of these transitions gives (i) associative substitution of strong π-acceptor/weak σ-donor ligands (^{13}CO, C_2H_4, and C_5H_{10}) but not N_2 or 2-MeTHF for CO at 90 K and (ii) inefficient photofragmentation in fluid solutions containing added ligands. The first allowed electronic transitions of $Os_3(CO)_{12}$ and $Fe_3(CO)_{12}$ give no photochemistry at 90 K and yield both fragmentation and substitution for $Fe_3(CO)_{12}$ in fluid solution. This transition is predicted[41] to exhibit characteristics intermediate between those of the $\sigma \rightarrow \sigma^*$ and $\sigma^{*\prime} \rightarrow \sigma^*$ states. Photochemistry associated with this transition for $Os_3(CO)_{12}$ is complicated at 298 K as a result of overlapping higher energy features which may, or may not, in fact be responsible for the inefficient long wavelength photofragmentation and photosubstitution behavior observed.[24,60]

Relatively low quantum yields for photofragmentation of $M_3(CO)_{12}$ complexes have been interpreted to indicate that excited states and intermediates formed along the primary photoreaction coordinate efficiently decay back to $M_3(CO)_{12}$.[21-23,60] In the presence of excess CO, C_2H_4, or PPh_3, 298 K photoproduct distributions appear to be unaffected by the additional presence of added CCl_4 in the solution, suggesting that previously proposed diradical intermediates,[3,18] if formed, are too short lived to be trapped by this radical scavenger. For Ru, hard donor ligands have been shown to act as Stern–Volmer type quenchers[21,22] of the photofragmentation chemistry in the presence of CO or PR_3, without significantly affecting 313-nm photosubstitution efficiencies.[23] Such characteristics have lead to the proposed intermediacy[21-23] of a nonradical reactive isomer of $Ru_3(CO)_{12}$ (IV) which is capable of first-order return to the starting cluster or of capture by a $2e^-$ donor, eq 9. Competitive loss of L from IV′ regenerates starting material.[23] Fragmentation rates for intermediate IV′, inferred from flash photolysis kinetic data,[23] were estimated to fall in the sequence CO, C_2H_4 >>> PPh_3.

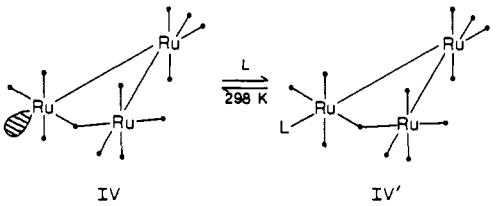

IV IV′ (9)

For broad band irradiation of $Ru_3(CO)_{12}$, photofragmentation predominates in reactions of $Ru_3(CO)_{12}$ with CO, PPh_3, and alkenes at 298 K. At 90 K, photoisomerization of axial-^{13}CO–$Ru_3(CO)_{11}(^{13}CO)$ to equatorial-^{13}CO–$Ru_3(CO)_{11}(^{13}CO)$ is rapid compared to CO loss and may proceed via a similar intermediate (IV). For Os photosubstitution dominates at 298 K, and selective loss of only ^{12}CO is observed for irradiation of axial-^{13}CO–$Os_3(CO)_{11}(^{13}CO)$ at 90 K.

The present study shows that, in accord with the flash kinetic data at 298 K, the long wavelength photochemistry of $Ru_3(CO)_{12}$ at 195 K is dominated by the nature of the $2e^-$ donor employed to scavenge intermediates. Long wavelength photoexcitation (λ > 420 nm) of $Ru_3(CO)_{12}$ at 195 K leads almost exclusively to photofragmentation [$Ru(CO)_4L + Ru_2(CO)_8L$] in the presence of added L = CO or C_2H_4 but not in the presence of added PPh_3. Less efficient (by at least one order of magnitude for 436-nm excitation) photogeneration of CO-bridged intermediate X results for L = PPh_3; retention of the Ru_3 framework is suggested by the thermal reactions of intermediate X to form $Ru_3(CO)_{12}$ and $Ru_3(CO)_{11}(PPh_3)$. Importantly, the absence of $Ru(CO)_4(PPh_3)$ as an initial 195 K photoproduct (i) is consistent with previous proposals[22] for the initial existence of a reactive Ru_3 intermediate and (ii) rules out other proposals[20] that the fragmentation of $Ru_3(CO)_{12}$ occurs via the simultaneous cleavage of two metal–metal bonds to form $Ru(CO)_4$ and $Ru_2(CO)_8$. Photofragmentation of $Os_3(CO)_{12}$[24,60] is also more efficient in solutions containing C_2H_4 vs. PPh_3. While the activation barrier for conversion of IV′ to $Ru(CO)_4L$ and $Ru_2(CO)_8L$ may be higher for a stronger σ-donor (weaker π-acceptor) ligand owing to the electron-withdrawing character of the bridging CO of this intermediate,[23] structural variations in IV′ may also be important. As with $M_3(CO)_{11}L$ complexes, strong π-acceptors may prefer equatorial coordination while weak π-acceptors may prefer axial coordination in IV′. While the $Ru_3(CO)_{12}$ complex fragments at 195 K to yield $Ru_2(CO)_8(C_2H_4)$ and $Ru(CO)_4(C_2H_4)$ in C_2H_4-containing solutions at 195 K, the products obtained in the long wavelength photofragmentation of $Fe_3(CO)_{12}$ at 298 K would be consistent with the initial formation of $Fe(CO)_5$ and $Fe_2(CO)_7(L)_2$ or, alternatively, $Fe_2(CO)_9$ and $Fe(CO)_3(L)_2$; $Fe_2(CO)_9$ is known to react with PR_3 (R = alkyl) to yield $Fe(CO)_5$, $Fe(CO)_4(PR_3)$, and $Fe(CO)_3(PR_3)_2$ complexes.[61] The difference in the long wavelength photofragmentation products for $Fe_3(CO)_{12}$ and $Ru_3(CO)_{12}$ may be associated with the different electronic nature of the lowest energy absorptions for these two complexes.

The wavelength dependent bimolecular photoreaction efficiencies at 90 K suggest the dominant intermediacy of $Ru_3(CO)_{11}$ in the photogeneration of $Ru_3(CO)_{11}(N_2)$ and $Ru_3(CO)_{11}$(2-MeTHF) complexes. However, the efficiencies suggest involvement of a second, transient intermediate or excited state responsible for the longer wavelength photogeneration of $Ru_3(CO)_{12-n}(^{13}CO)_n$ and $Ru_3(CO)_{11}(\eta^2$-alkene) complexes. These results suggest the long wavelength photogeneration of a reactive isomer of $Ru_3(CO)_{12}$, perhaps IV, which reacts with L to form an $Ru_3(CO)_{12}L$ adduct, perhaps IV′, at 90 K. Thermodynamic and/or cage effects suppress fragmentation of IV′ in favor of competing ligand loss (CO or L) to yield the substitution product or to regenerate $Ru_3(CO)_{12}$, respectively. The entering group dependence would again reflect the notion that net reaction from IV′ is related to the ability of L to stabilize IV′ through π-backbonding. Competitive accumulation of axially vacant $Ru_3(CO)_{11}$ accompanies higher energy excitation. For $Fe_3(CO)_{12}$ and $Os_3(CO)_{12}$,[24] ligand dependent associative photosubstitution is associated with the second allowed electronic transition while higher energy excitation yields $M_3(CO)_{11}$.

Implications for Catalysis. Research in this group and elsewhere has previously established that near-UV photolysis of $Fe(CO)_5$[5,62-64] or low energy visible light excitation of $Fe_3(CO)_{12}$[3,5] or $Ru_3(CO)_{12}$[3,4] in the presence of alkenes yields extraordinarily active alkene isomerization catalysts. Quantum yields for photocatalyzed isomerization of 1-pentene to *cis*- and *trans*-2-pentene

(60) Pöe, A. J.; Sekhar, C. V. *J. Am. Chem. Soc.* **1986**, *108*, 3673–3679.

(61) Braterman, P. S.; Wallace, W. J. *J. Organomet. Chem.* **1971**, *30*, C17–C18.

(62) Schroeder, M. A.; Wrighton, M. S. *J. Am. Chem. Soc.* **1976**, *98*, 551–558, Schroeder, M. A.; Wrighton, M. S. *J. Organomet. Chem.* **1977**, *128*, 345–358.

(63) Chase, D. B.; Weigert, F. J. *J. Am. Chem. Soc.* **1981**, *103*, 977–978.

(64) Whetten, R. L.; Fu, K.-J.; Grant, E. R. *J. Am. Chem. Soc.* **1982**, *104*, 4270–4272.

have been reported to exceed unity by two or three orders of magnitude at ambient temperature. These and other findings[20,29] are consistent with the notion of thermal catalytic processes subsequent to the photochemical generation of the actual catalyst. By using $Fe(CO)_5$ as the precursor, a carbonyl-bridged diiron complex[65] and, alternatively, a mononuclear tricarbonyl iron unit[62,64] have been proposed to carry the catalytic cycle. Iron–carbonyl intermediates have been observed at subambient temperature, including $HFe(CO)_3(\eta^3\text{-}C_3H_5)$ from photolysis of $Fe(CO)_4(C_3H_6)$ in a rigid alkane glass at 77 K.[66] In neat 1-pentene, warmup of photogenerated $HFe(CO)_3(\eta^3\text{-}C_5H_9)$ (from $Fe(CO)_5$ and 1-pentene at 77 K) results in significant catalytic isomerization of 1-pentene above 260 K in the dark. Eventual regeneration of $Fe(CO)_4$(alkene) is accompanied by decline of catalytic activity. $Fe(CO)_3(\eta^3$-allyl) radical species, also detected in 1–3% yield as photoproducts of $Fe(CO)_5$ and olefins, have been implicated in catalytic reactions of olefins.[67]

In C_2H_4-saturated alkane solution, visible irradiation of $Fe_3(CO)_{12}$ yields 1 equiv each of $Fe(CO)_5$, $Fe(CO)_4(C_2H_4)$, and $Fe(CO)_3(C_2H_4)_2$. Addition of deoxygenated 1-pentene to solutions of $Fe(CO)_3(C_2H_4)_2$, but not $Fe(CO)_4(C_2H_4)$ or $Fe(CO)_5$, results in rapid catalytic isomerization at 298 K to a mixture of 2-pentenes.[29] Estimated turnover rates for the long wavelength photocatalysis (700–900 min^{-1}) by $Fe_3(CO)_{12}$[5] are in close agreement with the turnover rates associated with the thermal catalysis by 1 equiv of $Fe(CO)_3(C_2H_4)_2$ at 298 K (600 min^{-1}). While catalytically active mononuclear species have been implicated based on good chemical yields of mononuclear photoproducts during long wavelength photoexcitation of $M_3(CO)_{12}$ (M = Fe, Ru) in alkene-, CO-, or phosphine-containing solutions,[3] present results provide the first direct evidence that a mononuclear tricarbonyl unit, present as a substitutionally labile $Fe(CO)_3(\eta^2\text{-alkene})_2$ complex, carries the catalytic cycle for alkene isomerization, photocatalyzed by $Fe_3(CO)_{12}$. Higher turnover rates have been estimated from near-UV excitation of $Fe(CO)_5$,[5] suggesting involvement of additional catalytic species. Mononuclear dicarbonyl species may be important as suggested by the catalytic activity found when 1-pentene is added to a solution of $Ru(CO)_2(C_2H_4)_3$.[29] Importantly, near-UV irradiation of $Fe(CO)_3(C_2H_4)_2$ in C_2H_4-containing alkane glasses at 90 K rapidly yields $Fe(CO)_2(C_2H_4)_3$ and eventually a monocarbonyl species formulated as $Fe(CO)(C_2H_4)_4$; these complexes rapidly back react with liberated CO at higher temperatures.[29]

While long wavelength ($\lambda > 420$-nm) photoexcitation of $Ru_3(CO)_{12}$ in C_2H_4-saturated alkane solutions at 298 K yields catalytically inactive $Ru(CO)_4(C_2H_4)$ according to eq 10, similar

$$Ru_3(CO)_{12} \xrightarrow[\text{alkane, 298 K}]{h\nu\ (\lambda > 420\ \text{nm}),\ C_2H_4} 3Ru(CO)_4(C_2H_4) \quad (10)$$

irradiation in the presence of 1-pentene yields photocatalytic isomerization to a mixture of 2-pentenes.[26] At 195 K, $Ru(CO)_4(C_2H_4)$ is the only observed mononuclear product, even after significant fragmentation of photogenerated $Ru_2(CO)_8(C_2H_4)$ has occurred. Under these conditions $Ru(CO)_5$ and $Ru(CO)_3(C_2H_4)_2$ are stable but are not accumulated. Photogenerated $Ru(CO)_5$ and $Ru(CO)_3(C_2H_4)_2$, if formed at 298 K, would not accumulate in C_2H_4-saturated solutions due to their facile conversion to $Ru(CO)_4(C_2H_4)$ according to eq 11 and 12. Future investigations should address the possibility that $Ru_2(CO)_8$(alkene) or $Ru_3(CO)_{12}$(alkene) intermediates fragment differently when the alkene is more bulky and/or contains allylic hydrogens.

$$Ru(CO)_5 + C_2H_4 \rightarrow Ru(CO)_4(C_2H_4) + CO \quad (11)$$

$$Ru(CO)_3(C_2H_4)_2 + CO \rightarrow Ru(CO)_4(C_2H_4) + C_2H_4 \quad (12)$$

Acknowledgment. This work was supported by the National Science Foundation.

Supplementary Material Available: IR and UV–vis spectral data for relevant complexes to supplement Table I; figures showing IR spectral changes associated with preparing $Ru_3(CO)_{11}(N_2)$ and axial-^{13}CO–$Ru_3(CO)_{11}(^{13}CO)$ from photogenerated $Ru_3(CO)_{11}$ at <110 K; figure showing IR spectral changes for the long wavelength photoconversion of $Ru_3(CO)_{12}$ to a mixture of $Ru(CO)_4(C_2H_4)$ and $Ru_2(CO)_8(C_2H_4)$ at 195 K; figure showing IR spectral changes for the long wavelength photoconversion of $Fe_3(CO)_{12}$ to a mixture of $Fe(CO)_5$, $Fe(CO)_4(C_2H_4)$, and $Fe(CO)_3(C_2H_4)_2$ at 298 K (10 pages). Ordering information is given on any current masthead page.

(65) (a) Swartz, G. L.; Clark, R. J. *Inorg. Chem.* **1980**, *19*, 3191–3195.
(66) Mitchener, J. C.; Wrighton, M. S. *J. Am. Chem. Soc.* **1983**, *105*, 1065–1067.
(67) Krusic, P. J.; Briere, R.; Rey, P. *Organometallics* **1985**, *4*, 801–803.